universität wien

MASTERARBEIT / MASTER'S THESIS

Titel der Masterarbeit / Title of the Master's Thesis

„Development and Validation of a Serpent-2 model for the TRIGA Mark II reactor of the Technical University Vienna“

verfasst von / submitted by

Henriette Herzog, BSc BSc

angestrebter akademischer Grad / in partial fulfilment of the requirements for the degree of

Master of Science (MSc)

Wien, 2017 / Vienna, 2017

Studienkennzahl lt. Studienblatt / degree programme code as it appears on the student record sheet:	A 066 876
Studienrichtung lt. Studienblatt / degree programme as it appears on the student record sheet:	Masterstudium Physik
Betreut von / Supervisor:	Ao.Univ.Prof.i.R. Dipl.-Ing. Dr.techn. Helmuth Böck

Masterarbeit

Development and Validation of a Serpent-2 model for the TRIGA Mark II reactor of the Technical University Vienna

von

Henriette Herzog, BSc BSc

unter der Anleitung von:

Ao.Univ.Prof.i.R. Dipl.-Ing. Dr.techn. Helmuth Böck
und

Marcella Cagnazzo, MSc

Abstract

The aim of this work the development and validation of the Technical University of Vienna TRIGA Mark II research reactor by means of the SERPENT II Monte Carlo Code. Using this Serpent model, the neutron flux was calculated in several in-core positions and compared with data from previous flux measurements and MCNP calculations.
Subsequently, irradiation experiments were simulated to benchmark the Serpent burn-up results with available experimental data. As a result fission products activity inventory and burn-up values were evaluated for selected irradiated fuel elements. An additional out of core experiment consisting in irradiation of fissile and fertile material foils, was also simulated with the current Serpent reactor model.
The burn up of individual fuel rods was finally determined.

Zusammenfassung

Ziel dieser Arbeit ist die Entwicklung und Überprüfung eines Computer Modells vom TRIGA Mark II Forschungsreaktor der Technischen Universität Wien mit den neu entwickelten Simulationsprogramms Serpent II. Mit den Serpent Modell wurde der Neutronenfluss an mehren Positionen im Reaktorkern simuliert und mit Daten aus vorangegangen Fluss Experimenten und MCNP Simulationen verglichen.
Danach wurden mehrere Bestrahlungsexperimente simuliert um die Abbrand Berechnungen von Serpent mit experimentellen Daten zu überprüfen. Dabei wurde die Aktivität der Spaltprodukte und die Abbrand Daten für einige Brennstäbe des Reaktors bestimmt. Außerdem wurde noch ein Experiment im Kern simuliert, bei welchen Folien aus spaltbaren Material bestrahlt wurden.
Als letztes wurde der Abbrannd der einzelner Brennstäbe bestimmt.

Acknowledgement

First I want to express my sincere gratitude to my supervisor Marcella Cagnazzo for her support during the time I worked on this master's thesis. I am very grateful for her patience, dedication and support.
I would also like to thank Helmuth Böck for his guidance through the process of this thesis and for the opportunity to work on this topic. Many thanks as well go to Mario Villa and Thomas Stummer for their help and support and to Jaakko Leppänen and his team for their technical support while working with the Serpent code.
Finally I would like to thank my family and friends for their support and encouragement.

Contents

Introduction

In Physics, computer simulations help to find solutions for complex systems, such as a nuclear reactor. These simulations fill the gap to theory, where often solutions for basic problems only can be found experimentally. Computer simulations are often used in nuclear reactor physics, because they are a good tool to understand and show the processes in a reactor. Because of the complexity, geometry and safety aspects it is often not possible to perform an experiment in a reactor. Here computer models help out, for example inside a fuel element.

Stochastic neutronics modelling, in particular the Monte Carlo method for neutron transport, have been used for decades in reactor physics and bring good results. A good example for a proved and widely used code is the MCNP (Monte Carlo N-Particle Transport Code) developed in 1957 by the Los Alamos National Laboratory [1]. These code is used since years at the Atominstitut of the Technical University in Vienna.

In the year 2004 a new code development stared at the VTT Technical Research Centre of Finland. This new code Serpent based also on the principle of Monte Carlo routines. This code can be also used for burn up calculations [2].

The TRIGA Mark II research reactor in Vienna is the only research reactor in Austria. The history of this reactor is long but the reactor is important to train and educate physicists in Austria. The reactor was built in the sixties. In the year 2012 the fuel elements in the reactor core were exchanged.

The aim of this work is to simulate the TRIGA Mark II reactor in Vienna with the new reactor physics code Serpent and to estimate the transmutation rates (production and depletion) of the fuel elements in the reactor. To validate the Serpent Code the results for the neutron energy spectrum were compared with previous codes.
An another way to validated the Serpent code was to compare the simulation with exper-

iments. This tasks contains a irradiation of foil samples of natural uranium and natural thorium in the TRIGA Mark II reactor in Vienna. Also burn up calculation of different fuel elements were carried out. This data were compared with experimental data of gamma spectroscopy of several fuel elements.
The results of the Serpent simulation were compared to experimental data. This experiments were carried out before and presented in different thesis [3; 4].

After the validation of the code, different burn up calculation were carried out to estimate the TRIGA fuel composition. Also the burn up of the fuel elements was determined by the simulations.

With this combined data it can be shown that the new Monte Carlo code Serpent is a useful tool in reactor physics and it provides data of the nuclide determination of the fuel elements. The first part of this work describes theoretical reactor physics, the TRIGA Mark II reactor of Vienna and offers an introduction to the Serpent code. The second part depicts the Serpent model for the TRIGA reactor in Vienna, the validation and the burn up simulations.

Part I

Background

Chapter 1

Reactor Physics

An atom consists of protons, neutrons and electrons. Protons and neutrons are located in the atomic nucleus. Electrons are in shells around the core. Protons are positively charged and electrons negatively, both with the value of the elementary charge ($e = 1,60218 \times 10^{-19}$ C).

Individual elements differ by their different numbers of protons. The proton number is Z, N is the number of neutrons in the atom. The mass number A of the atom is the sum of both:

$$A = Z + N \tag{1.1}$$

Nuclides with the same proton number, but with different neutron numbers are called isotopes. The masses of protons (in the order of 10^{-27} kg) and neutrons are nearly equal. The mass of an electron is negligible (order of 10^{-31} kg). The notation of a nuclide is ${}^{A}_{Z}X$ or $X - A$, where X is the element symbol [5].

1.1 Neutrons

Neutrons not bound to an atomic nucleus have a lifetime of about only approximately 15 minutes. They decay into a proton, an electron and an anti-neutrino. Nevertheless, they can move through matter and possess a certain kinetic energy. These free neutrons are divided into groups by means of kinetic energy. The classification of the neutrons in the following table 1.1.1 is selected in such a way that the results of the simulations can be compared later.

Group	Energy range [MeV]
thermal neutrons	$< 6.9 \times 10^{-7}$
epithermal neutrons	6.9×10^{-7} - 0.11
fast neutrons	> 0.11

Table 1.1.1: Classification of neutrons

1.2 Binding Energy

Einstein's equation provides a connection between energy and mass.

$$E = m \cdot c^2 \tag{1.2}$$

c is the velocity of light.

The total mass of a nuclide is lighter than the sum of the individual components, because the binding energy has to be deducted.

$$m_{nucleus} = Zm_p + Nm_n - \Delta m_{nucleus} \tag{1.3}$$

$\Delta m_{nucleus}$ is called the mass defect. With Einstein's equation 1.2 the mass defect can be converted into the binding energy. The binding energy is set free by the creation of the core and has to be supplied by fragmenting the core. The formula of the binding energy was found empirically by H. Bethe and C. F. Weizsäcker.

$$E_{binding} = a_v A - a_O A^{2/3} - a_c \frac{Z^2}{A^{1/3}} - a_a \frac{(N-Z)^2}{A} \pm a_p A^{-2/4} \tag{1.4}$$

Regarding the coefficients a : a_v is the volume term, a_C the coulomb term, a_O the surface-factor, a_a the asymmetry term and a_p is called the pairing term, which is positive if N and Z are even numbers and negative if N and Z are odd, and otherwise zero.
The following figure 1.2.1 shows the binding energy of different nuclides, also the mean results of the binding energy are described [5; 6].

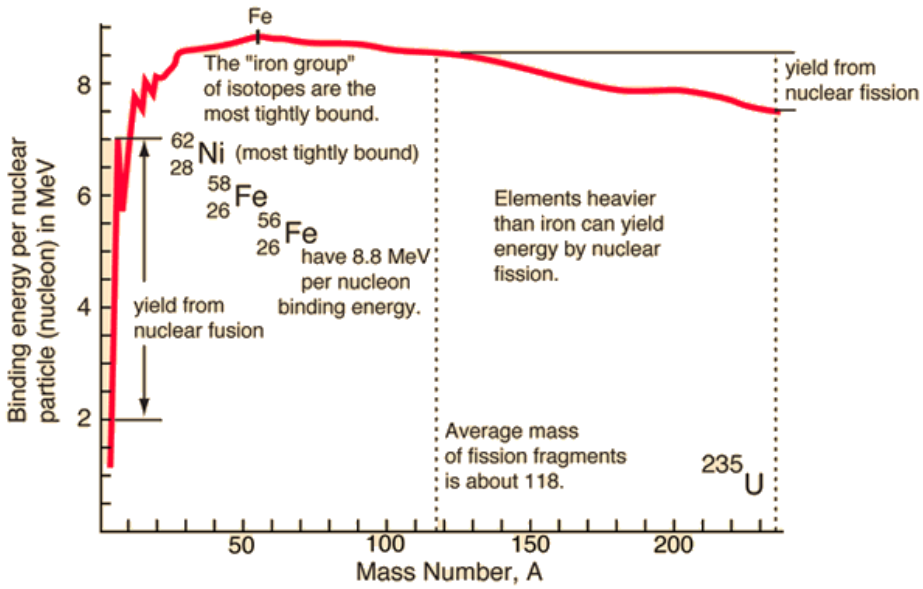

Figure 1.2.1: Binding energy per nucleon as a function of the mass number A. The light nuclides are, where the binding energy is low, able to preform nuclear fusion. Isotopes of iron are the most stable, as they have the highest binding energy. For heavier nuclides the binding energy decreases and fission can happen [7].

1.3 Radioactive Decay

If the binding energy is low enough, nuclides can decay. A nuclide decays into another nuclide, a process which is called radioactive decay. There are different types of radioactive decay, described shortly in the following sections. The nuclide which decays is called mother-nuclide (X) and the developed nuclide daughter-nuclide (Y) [5].

1.3.1 α-Decay

During α-decay, a heavy nuclide decays to a lighter nuclide by emitting an α-particle. The α-particle is a helium-nucleus, consisting of two protons and two neutrons. It is doubly positively charged.

$$ {}^{A}_{Z}X \rightarrow {}^{A-4}_{Z-2}Y + {}^{4}_{2}He^{++} \tag{1.5} $$

In order for an α-particle to be emitted from the nuclide, a coulomb-potential has to be overcome. This is only possible by quantum tunnelling. The energy set free by the mass defect is used for the kinetic energy of the α-particle and the daughter-nuclide [5; 8; 9].

1.3.2 β-Decay

During β-decay the mass-numbers of the nuclides are not changed. It is caused by the weak interaction. There are different types of β-decay.

1.3.2.1 β^--decay

The isotope has a neutron surplus. A neutron of the nucleus converts into a proton by emitting an electron and an anti-neutrino.

$$n \rightarrow p + e^- + \bar{\nu} \tag{1.6}$$

The nuclear reaction for this process is written as:

$$^{A}_{Z}X \rightarrow ^{A}_{Z+1}Y + e^- + \bar{\nu} \tag{1.7}$$

1.3.2.2 β^+-decay

For isotopes with a proton surplus, the decay process is β^+. A proton of the core converts into a neutron by emitting a positron and a neutrino.

$$p \rightarrow n + e^+ + \nu \tag{1.8}$$

The nuclear reaction for this process is written as:

$$^{A}_{Z}X \rightarrow ^{A}_{Z-1}Y + e^+ + \nu \tag{1.9}$$

The lifetime of the positron is short, it annihilates with an electron by emitting two photons in opposite directions with an energy of 511 keV each.
The minimal energy difference between mother and daughter nuclide-mass is 1022 MeV for the β^+decay.
The energy spectrum of the β-decay is continuous, because the release energy is split in the kinetic energy of the electron and anti-neutrino by β^--decay (or positron and neutrino for the β^+-decay) [5; 8; 9].

1.3.2.3 Electron Capture

If the energy difference is less than 1022 MeV the decay mode is electron capture. For higher energy differences electron capture is an alternative to β^+-decay.
By electron capture, a proton of the nucleus captures an electron from an inner shell (mostly the K-orbital) and combines with it to from a neutron by emitting a neutrino.

$$p + e^- \rightarrow n + \nu \tag{1.10}$$

The total nuclide mass is not changed in this process.

$${}^{A}_{Z}X \rightarrow {}^{A}_{Z-1}Y + \nu \tag{1.11}$$

The vacant position of the inner orbital is filled by an electron from an outer orbital by emitting one or more characteristic X-rays. Sometimes the excessive energy of this process is committed to an electron in an outer shell, which is then emitted as a so-called Auger-electron [5; 8; 9].

1.3.3 γ-Radiation

In the transition from an excited state to the ground state (or lower excited state) of the nuclide, an electromagnetic wave with a characteristic wavelength is emitted. The energy of the wave depends on the energy gap between the two states.

$$E_\gamma = h\nu = E_1 - E_2 \tag{1.12}$$

E_1 is the energy of the higher excited level and E_2 the energy of the lower level, h is the Planck's constant and ν the frequency of the emitted wave. By γ-decay no element conversion (as by α- or β- decay) takes place. But often emission of γ-radiation is the result of a previous decay [5; 8].

1.4 Nuclear Fission

Very heavy nuclides (Z>90) can split into two medium heavy nuclides if the nuclear force is overcome. This process is called nuclear fission. To split a nuclide an input energy is necessary. This energy is usually around 6 MeV, slightly differnt for each isotope, can be overcome and the nuclides splits.

There are two types of nuclear fission, the first one is spontaneous fission. In the case of spontaneous fission a very heavy nuclide splits without any external impact, the reason for this is quantum tunnelling. This process is very rare, α-decay is more likely. The second process is the induced fission, occurring in a nuclear reactor. A neutron attaches onto a nuclide which then finds itself in an excited state. For example:

$$^{235}U + n \rightarrow (^{236}U)^{*} \tag{1.13}$$

The energy of the nuclide in the excited state is now increased by the binding energy of the neutron and kinetic energy with which the neutron hit the nuclide. In the case of $^{236}U^{*}$ the energy is high enough to overcome the binding energy and the uranium-isotope splits into two fission products. Several channels for the fissions are possible. The mass distribution of the fission products are shown in the following figure 1.4.2.

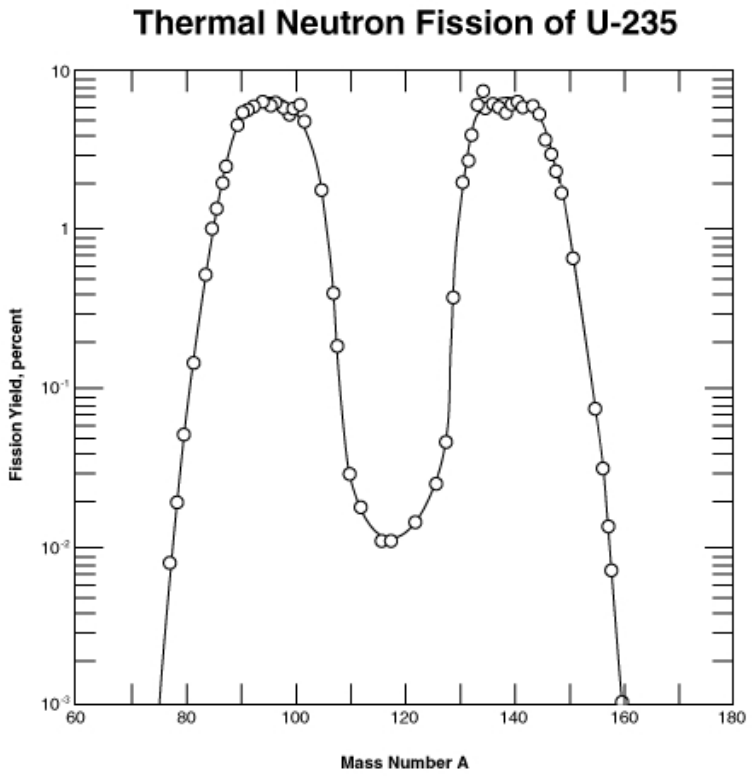

Figure 1.4.2: Fission Yield of the fission products by the fission of U-235 by thermal neutrons [10]

The binding energy of the neutron with ^{235}U to $^{236}U^{*}$ is already high enough for fission.

There is therefore no need for the kinetic energy, and fission can be induced by thermal neutrons. This is the reason why ^{235}U is used in reactors.
During the fission process, 2-3 neutrons are always released, these are fast neutrons. They are called prompt neutrons, since they are released directly during cleavage. The energy spectrum of these prompt neutrons corresponds to a Maxwell Distribution.

The fission products are mostly radioactive, because of their neutron spill over. They decay in a β^-- chain. In some cases of β^-- decay the energy of the excited state is so high, that instead of a γ-quantum, a neutron is emitted. These neutrons are called delayed neutrons. Prompt neutrons are emitted 10^{-14} s after fission, delayed neutrons between milliseconds and minutes after fission. Although the ratio of delayed neutrons compared to the total emitted neutrons during a nuclear fission is small, they are important to be able to control the reactor.
A chain reaction occurs if the same or a higher number of neutrons are emitted than absorbed during a nuclear fission process [5; 6; 9].

1.5 Radioactive Decay Law

The total number of nuclides of an isotope decreases over time. The factor responsible for this change is called the decay constants λ. The number of nuclides which exist after a time t can be calculated from the number of nuclides at time $t = 0$ with an exponential decay:

$$N(t) = N_0 \cdot e^{-\lambda t} \tag{1.14}$$

The decay is a statistic process, so it is not possible to predict, which nuclide decays next, but it is possible to say how many nuclides have decayed in a certain time. The time after which half of the original nuclides have decayed is called the half-life.

$$\frac{N_0}{2} = N_0 \cdot e^{(-\lambda T_{1/2})} \tag{1.15}$$

$$T_{1/2} = \frac{\ln(2)}{\lambda} \tag{1.16}$$

The half-life and thus also the decay constant is different for every isotope. It also can be used to characterise isotopes. The number of decays within a certain time is called Activity A. The unit of Activity is *Becquerel* (Bq), 1 Bq corresponds to one radioactive decay per second.

$$A = \lambda \cdot N = A_0 \cdot e^{-\lambda t} \tag{1.17}$$

Often isotopes do not decay directly into a stable nuclide, but into another radioactive isotope which decays as well. This is called a decay chain. The first isotope which decays is called mother and the second, daughter. If there is only the mother isotope present at $t = 0$ with a number N_{10}, it will decay and produce a daughter nuclides. However, the daughter nuclides will also decays themselves. To get the numbers of daughter nuclides at a time t (N_2), production of the isotopes during the decay of the mother and daughter isotopes have to be considered.

$$N_2(t) = N_{10} \frac{\lambda_1}{\lambda_2 - \lambda_1} (e^{-\lambda_1 t} + e^{-\lambda_2 t}) \tag{1.18}$$

With only a mother and a daughter nuclide, it is a two-chain decay. With more than two decays in the chain formula 1.18 becomes more complicated [5; 8].

1.5.1 Cross Section

The cross section σ describes the probability of an interaction with the nuclide. It is the ratio between the reaction at one nucleus and the total number of particles hitting the target area. It is the microscopic cross section, defining an area that is hit by the particle beam. It has the dimension of area, in the order of 10^{-24} cm^2.
The microscopic cross section refers to a single atom. The macroscopic cross section Σ however refers to a volume, by multiplying the microscopic cross section with the total number of atoms (N) per volume.

$$\Sigma = \sigma \cdot N \tag{1.19}$$

N can be found by using the mass or atomic density of the isotope. The unit of the macroscopic cross section is $[cm^{-1}]$.

The total cross section σ describes any type of interaction, this contains elastic and inelastic scattering as well as any type of nuclear reaction. The total cross section is the sum of the different types of cross sections including [6]:

- σ_a cross section for absorption
- σ_e cross section for elastic scattering

- σ_i cross section for inelastic scattering
- σ_γ cross section for radiation capture
- σ_f cross section for fission

The cross section strongly depends on the kinetic energy of the incoming particle, in a nuclear reactor the incoming particle is a neutron. In the following figure 1.5.3 the fission cross section of U-235 is shown, dependent on the energy of the incoming neutron.

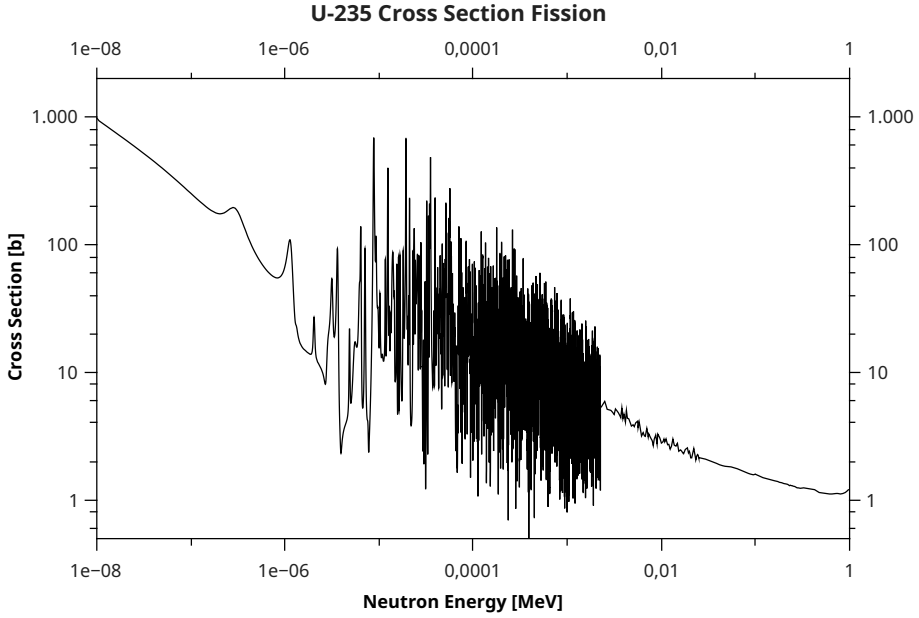

Figure 1.5.3: Cross section generated from the data library ENDF/B-VII.1 [11]

1.6 Moderation and Interaction of Neutrons

When neutrons move through matter, different reactions can occur.
Scattering processes play a significant role in the movement of neutrons through matter. In the simplest way a neutron hits the target (an isotope) and after collision, only changes direction, its kinetic energy being conserved. This only happens if the kinetic energy of the neutron is low, as with thermal neutrons. At higher energies inelastic scattering can occur. Here the kinetic energy of the incoming neutron is not conserved. After the collision the direction of the neutron has changed as well as its kinetic energy being lower. The lost energy now is transmitted to the target particle. The absorbed energy is emitted via γ-radiation.

During the process of inelastic scattering the neutron slows down. This is called moderation.

Besides scattering processes another reaction can take place, such as capture. It occurs when an incoming neutron is bound to the target nuclide. This often causes a reaction afterwards. For example in the case of radiative neutron capture (n, γ), if the target captures the incoming neutron, it is then in an excited state and by transmitting γ-radiation it falls back to the ground state. For example:

$$^{238}U + n \longrightarrow ^{239}U^{*} \longrightarrow ^{239}U + \gamma$$

An (n,α)-reaction causes an α-particle to be emitted, in the case of an (n,p)-reaction, a proton, and (n,He-3)- reactions lead to the emission of a Helium-3 nucleus. Besides capture reactions, a neutron can also induce fission, written as (n,f)-reaction.

Fission and moderation are the two main processes used to regulate a reactor [6; 12].

1.7 Chain Reaction

For the operation of the nuclear reactor, neutrons are emitted from a starter source and decelerated by the water, which acts as moderator. If thermal neutrons hits the fuel material fission can take place. If, as a result of the fission, at least as many neutrons are released as have been absorbed, a chain reaction occurs. Only then is the operation of the reactor possible. This is described by the multiplication factor k.

$$k = \frac{\text{Neutrons of the generation i}}{\text{Neutrons of the generation i-1}} \tag{1.20}$$

If $k \geq 1$ a chain reaction occurs. If $k < 1$ no chain reaction occurs. The formula for determining the multiplication factor is the so called “Four-Factor-Formula”.

$$k_{\infty} = f_{th}\eta_{th}\epsilon p_{th} \tag{1.21}$$

The factors and their range are as follows:

- f_{th} is the *thermal utilization factor* and describes the ratio of absorbed thermal neutrons in the fuel to the total number of absorbed neutrons, $f_{th} < 1$
- η_{th} the *reproduction factor* is the number of fast neutrons that are generated during the fission per absorbed neutron, $\eta_{th} > 1$

- ϵ is the *fast fission factor*, this factor indicates how many fissions are triggered by fast neutrons, $\epsilon \geq 1$
- p_{th} the *resonance escape probability* is the probability that a neutron is not absorbed parasitically during braking. It is lost during an (n,γ)-process, $p_{th} < 1$

The Four-Factor-Formula 1.21 describes the multiplication factor in an infinite reactor. But reactors are limited by their geometry. So the k_∞ has to be multiplied by the probabilities of the non leaking of the neutrons of the system. This factors is called "non-leakage factors", there is one for thermal P_{th} and one for fast neutrons P_f

$$k_{eff} = k_\infty P_f P_{th} \tag{1.22}$$

if $k_{eff} = 1$ the reactor is critical, when $k_{eff} > 1$ it is said the reactor is supercritical and by $k_{eff} < 1$ subcritical and no chain reaction occurs [6].

1.8 Burn Up

Through the fission process during the reactor operation, the composition of the reactor fuel element changes. This change can be described by the burn up. Burn up is the realised (thermal) energy during the operation by the fuel relative to the mass of burnable material. The unit is MWd/kg. Burn up of a material can also be given in relative values. FIFA describes the fission per initial fissionable atoms, it is the ratio between burned material and originally available material, mostly given in percentages.

Chapter 2

TRIGA Mark II Vienna

The research reactor at the Technical University of Vienna/Atominstitut (ATI) is a type TRIGA Mark II reactor.
TRIGA is a type of research reactor used worldwide, produced by the company *General Atomic*, San Diego USA. TRIGA stands for *Training Research Isotope Production General Atomic* and the begin of the development of TRIGA reactors were in August 1955 [13].
After a large international conference in Geneva/Switzerland General Dynamics Corporation in San Diego, California was convinced to develop nuclear reactors and nuclear energy. 1956 *General Atomic Division* (now General Atomics, GA) was founded. In June 1956 the company commissioned a group of scientists to design a "safe" reactor. The aim of this reactor was to be safe, relatively inexpensive and allows different kinds of experiments. The sole engineering of safety applications was not enough, the reactor fuel itself should have inherent safety characteristics [13]. This meant that even if all control rods are removed abruptly from the core, the reactor should be in a stable condition without any damages to the fuel or the reactor [14].
In 1958 the first prototype of the TRIGA reactor became critical, and after ten years 32 reactors were installed worldwide [14]. Over the years the TRIGA reactor was refined, different fuel types which differ in cladding, enrichment, uranium amount and burnable poison were developed, also the reactor itself was advanced. In the end six design research reactor were devolped by the GA under the trademark TRIGA. All based on the first TRIGA design with an open-pool, light water moderation and a UZrH fuel elements [14].
Over 60 reactors were installed worldwide, in October 2016 38 of them are still in operation [13; 15; 16].

The reactor in Vienna was built from 1959 to 1962 by the company *General Atomic* and was

critical for the first time on the 7th of March 1962, after this date the reactor was in constant operation. The average operational time is about eight hours per day and 220 days per year [16].

The TRIGA Mark II design is an above ground reactor. The reactor tank is placed in a concrete shell, which is also the radial irradiation shielding. The fixed core consists of 76 fuel elements (FE), 3 control rods and 8 dummy graphite elements. The neutron source for this reactor is an Sb-Be photo neutron source. All reactor elements are desribed in more detail in section 2.2.
The core is surrounded by a graphite reflector with a depth of 30.5 cm and a hight of 55.9 cm. Between the core and the reflector is a rotary specimen rack containing 40 rotating irradiation positions for experiments and storage. This rack is called “Lazy Susan”.
Apart from the graphite reflector, the core is also shielded by water, in the radial direction this shield is at least 45.7 cm. Over the core, the water reaches 4.9 m hight and beyond the core 61 cm [14; 17]. The water tank is surrounded by an aluminium tank and a thick borate concrete structure [1].

The maximum continuous power of the TRIGA reactor in Vienna is 250 kW (thermal). After initialization it needs about one minute to reach this level. The design of this reactor fuel allows an operation in pulse mode. The moderation of the fuel is less efficiently at high temperatures so a pulse for a short time is possible. In this mode the power reaches 250 MW for a short time. The lifetime of the prompt pulse is 40 ms. Due to the negative temperature coefficient of the reactivity of the reactor fuel the power decreases shortly after the pulse to the normal level of 250 kW [14].
At normal power (250kW) the fuel temperature is around 200 °C in the centre, at pulse mode it reaches 360°C. The thermal neutron flux density increases from 1×10^{13} $cm^{-2}s^{-1}$ in normal operation to 1×10^{16} $cm^{-2}s^{-1}$ at 250 MW in the central irradiation tube. The thermal flux is in the central irradiation tube the highest. In the irradiation tubes the thermal flux is lower by the factor of 0.17 compare to the central tube.
The reactor is controlled by means of the three control rods. These can be moved individually. If all three control rods are in the lower position, they are at the same level as the fuel elements. In this position, the three control rods absorb all neutrons from the Sb-Be photo neutron source and the reactor is not critical and switched off.
If the control rods are withdrawn, the reactor starts. When all three are completely removed from the core, the reactor operates with the maximum power of 250 kW.
The temperature of the reactor is regulated by two separated cooling circuit. The primary

cooling circuit is filled with distilled, deionized water and is separate from the second circuits, which constitutes normal ground water by a heat changer. The temperature in the first cooling circuit is between 20 and 40 °C and the one of the second is between 12 and 18 °C. The reactor contains many different experimental facilities, inside the core, in the graphite reflector, in special tubes across the reflector, and others. For details see section 2.3 [1; 14; 16].

In order to satisfy the safety requirements, a fuel element was developed for the TRIGA reactor. For this purpose a material with a negative temperature coefficient was used. The material UZrH was selected for this purpose. It is a solid and through the hydrogen this fuel element also has moderator properties. The UZrH is a homogeneous mixture. The material proved to be very suitable, besides the negative temperature coefficients it also has a good heat capacity and a low reactivity with water. In the beginning high enriched uranium (HEU fuel elements) were used. But in the late 1970s fuel elements with low enriched uranium (LEU) were devolped to increase the core life. During the years disks of burnable poison were added to the fuel element also to increase the lifetime and to contribute to the temperature coefficient [14].
In the years since 1962 the Vienna TRIGA reactor operates with mixed fuel elements, like low enriched uranium (LEU) fuel and high enriched uranium (HEU) fuel elements. Because some of the fuel rods were already close to their maximum burn and the take back guarantee was approaching the end, it was decided to replace the fuel elements. The core conversion took place in November 2012.
The 27 of April 2012 was the last operation day with the old fuel elements. For the next six months the reactor was shut down, thereby allowing the fuel elements to cool down before their removal. In exchange for the 91 old fuel elements the Atominstitut in Vienna received 77 almost new fuel elements, 13 fresh or almost fresh elements staying at the reactor. These new fuel elements had previously been used by reactors in Japan and the USA. Due to their low burn up they were selected for further use in the TRIGA Reactor Vienna.
75 fuel elements came originally from the Musashi Reactor in Japan. These elements had a burn up of less than 1%. The two fuel elements from the reactor of Cornell University had a burn up slightly above 1%.
In the night from 29 to 30 of October 2012 the fuel elements arrived in Vienna. In the next week the old fuel elements were taken from the reactor and the new ones were stored. On the 7 of November the reactor core was built up, by adding one fuel element after another. The reactor was critical with 64 fuel elements.
Finally, the reactor core consisted of 76 fuel elements, of which 71 were from Japan and the

remaining five, fresh ones that had been stored at the Atominstitut up to this point in case some need to be exchanged.
After some shuffling of the Fuel elements and testing, the normal reactor operation was resumed on the 21 of January 2013 [18; 19].

2.1 Reactor tank

The reactor tank is made of aluminium. It is 6.4 m deep and the diameter is 1.98 m and filled with deionised distilled water. The core is located 4.9 m beneath the surface of the water.
The tank is surrounded by a nearly octagonal concrete wall. From the bottom up to a height of 3.6 m it consists of heavy concrete with a thickness of 2.08 m, above that of normal concrete with a thickness of 1.1 m. The cladding of the tank is a 6 mm thick and made of steel. A schematic cross section of the reactor tank is shown in figure 2.1.1 below. The graphite and the water provided a good shielding so it is possible to stand next to and on the reactor [20].

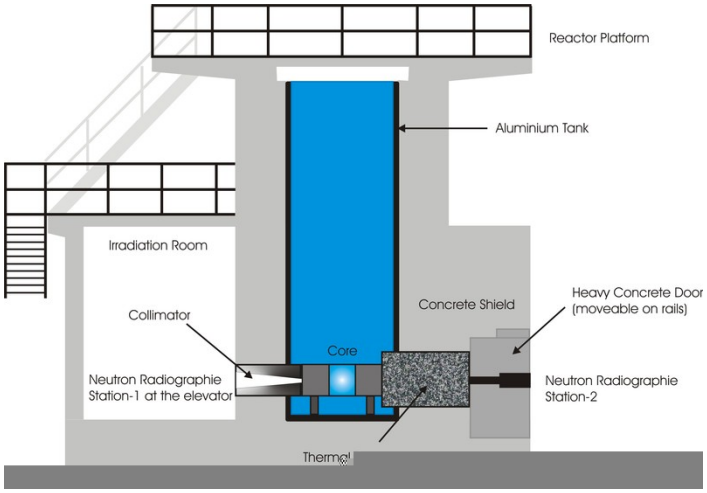

Figure 2.1.1: Cross section of the TRIGA MARK II Reactor in Vienna [21]

2.2 Reactor Core

The core consist of 90 elements arranged in an annular lattice in five rings around the central irradiation tube. The position of the central irradiation tube (CIT) is called A1. The rings are labelled with B, C, D, E and F. B is the inner ring and F the outer. In figure 2.2.2 the core lattice is shown with the core configuration of the year 2015.

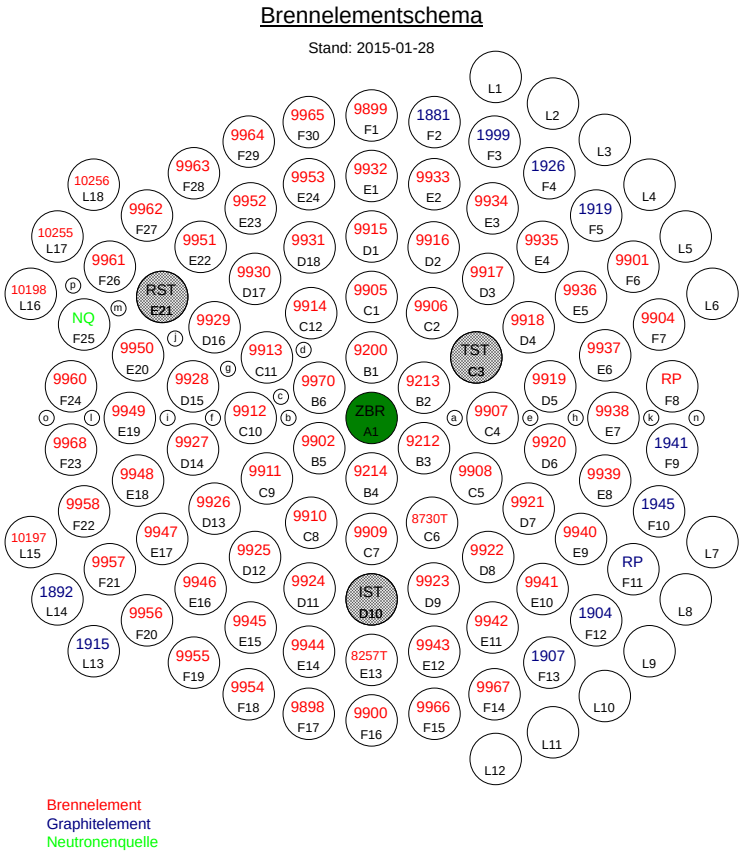

Figure 2.2.2: Core setting in the year 2015

The elements inside the core are fuel elements, control rods, dummy graphite elements and one neutron source. The core elements are held in position by two aluminium grid plates, one at the bottom and one at the top of the reactor core. The plates have a diameter of 4.5 cm and a thickness of 1.9 cm. Ninety holes, each with a diameter of 3.82 cm ensure exact spacing of the core components. There are also sixteen smaller holes in the plate, with a diameter of 8 mm, to insert samples.
All elements are described in detail in the following sections.

2.2.1 Control Rods

There are three control rods to control the power of the reactor. If all three of them are fully inserted they absorb all neutron emitted by the neutrons source, the reactor is sub-critical. The rods consist of powdered boron carbide (B_4C) covered by an aluminium cladding. The boron carbide is the absorber material. The rods are all 40 cm in length but the diameter of each is different. The safety-transient rod (IST) at the Position D10 has a diameter of 2.5 cm. The shim rod (TST) a diameter of 3.2 cm at the Position C3. And on Position E21 is the regulating rod (RST) with a diameter of 2.2 cm. Two of them are withdrawn by an electric motor, one by a pneumatic system. The start up process needs several minutes from sub-critical state up to a power of 250 kW. Shut-down requires 0.1 sec. It can be done either manually or automatically by the safety system [16; 20].

2.2.2 Fuel Elements

The core is loaded with 76 fuel elements. They are all the same type, 104 or SS-clad (which stands for stainless steel cladding). Each fuel element has a diameter of 3.75 cm and a length of 72.06 cm [1].

The fuel meat is a homogeneous mixture of Uranium-Zirconium-Hydride (U-ZrH), with 91.5 wt.% Zirconium-Hydride (ZrH) and 8.5 wt.% of low enriched Uranium. The enrichment of the Uranium is about 20%. The ZrH serves as moderator. The moderation performance of ZrH is temperature-dependent. It is lower at higher temperatures, therefore the reactor can be operated in pulse mode. The fuel meat is cylindrical around a pure Zr-rod, below the fuel meat is a disk of burnable poison of molybdenum. At the top and bottom of the fuel element a graphite element is situated. The entire fuel cylinder is covered with stainless steel. The specifications of the type 104 fuel element are listed in the table 2.2.1. [1; 16]

In two fuel elements thermocouples are implemented. These fuel elements are on the position C6 and E13. These specifications allows the measurement of the fuel temperature during reactor operation [20].

In 1996 the fuel element production was moved from the General Atomics in the USA to CERCA in Romans/France. Since then CERCA produces every type of TRIGA fuel from HEU to LEU. Currently the production is stopped to make post-Fukushima safety upgrades [13].

Fuel Meat	U-ZrH
Density [g/cm^3]	5.8624
Diameter [cm]	3.6449
average Mass [g]	2259.85
Length [cm]	38,1
Burnable Poison	Molybdenum disk
Density [g/cm^3]	1.28
Diameter [cm]	3.63
Thickness [cm]	0.02
Axial Reflectors	Graphite
Density [g/cm^3]	1,6
Diameter [cm]	3.63
Length upper reflector [cm]	6.8
Length lower reflector [cm]	9.31
Central Zr-rod	Zirconium
Density [g/cm^3]	6.49
Diameter [cm]	0.635
Length [cm]	38.1
Fuel Cladding	SS-304
Density [g/cm^3]	7.9
Thickness [cm]	0.051
Total Length [cm]	72.06
Total Diameter [cm]	3.75

Table 2.2.1: Details of fuel specification of type 104 fuel element [1]

2.2.3 Graphite elements

In the core, eight dummy graphite elements are, used to increase reactivity. If one graphite element is removed the reactivity decreases by 10 ¢. The graphite elements have the same dimensions as the fuel element, but consist of nuclear grade graphite surrounded by a thin Aluminium cladding [16].

2.2.4 Neutron Source

The cylindrical photoneutron source consists of an inner Antimony (Sb)-cylinder surrounded by a Beryllium (Be)-cylinder. The Sb-cylinder has a diameter of 1 cm and the thickness of the Be-cylinder is 0.5 cm. The total length of the source is 40.4 cm. 6×10^6 starter neutrons are emitted by the source per second [1].

2.3 Experimental Facilities

The TRIGA MARK II in Vienna is a research reactor designed for basic and applied nuclear research and education. There are thus many different facilities for neutron and γ-irradiation, isotope production and sample activation in the reactor. There is one Central Irradiation Tube (CIT) in the centre of the core, the diameter of which is 3.48 cm. Furthermore there are sixteen smaller tubes in the core for foils activation to determine the flux. The positions are marked in figure 2.2.2 with the letters a-p. In the reflector five irradiation tubes are inserted, the positions labelled LS 1-5 (for Lazy Susan, the rack in which they are inserted).

In the reactor are also two tubes for pneumatic delivery and four beam tubes to provide neutron beams for experiments.

The four beam tubes are called A, B, C and D. The tubes A, B and C are located radially to the core, A terminates at the inner surface of the reflector, also at the outer edge of the core, B and C terminate both at the outer end of the reflector. The tube D is tangential to the core. All tubes are located nearly 10 cm below the middle of the core and have a diameter of 15.24 cm. The tubes are for irradiation experiments and the tube A very close to the core to provide maximum exposure [14].

The thermal column is also a part of the radiation facilities, it supplies thermal neutrons for different experiments. The column is a 1.2 m $\times$ 1.2 m container with a depth of 1.6 m. It is a boral lined graphite, clad with aluminium [1; 16]. A pneumatic transfer systems provides fast transport of irradiated samples from the reactor to the chemistry laboratory. The fast pneumatic transfer system needs 20 ms for the transfer of a sample, the other 3 s. The position for the transfer tubes are F8 and F11 labelled in figure 2.2.2 with RP (german for "Rohrpost"). In the following figure 2.3.3 the radiation facilities are shown.

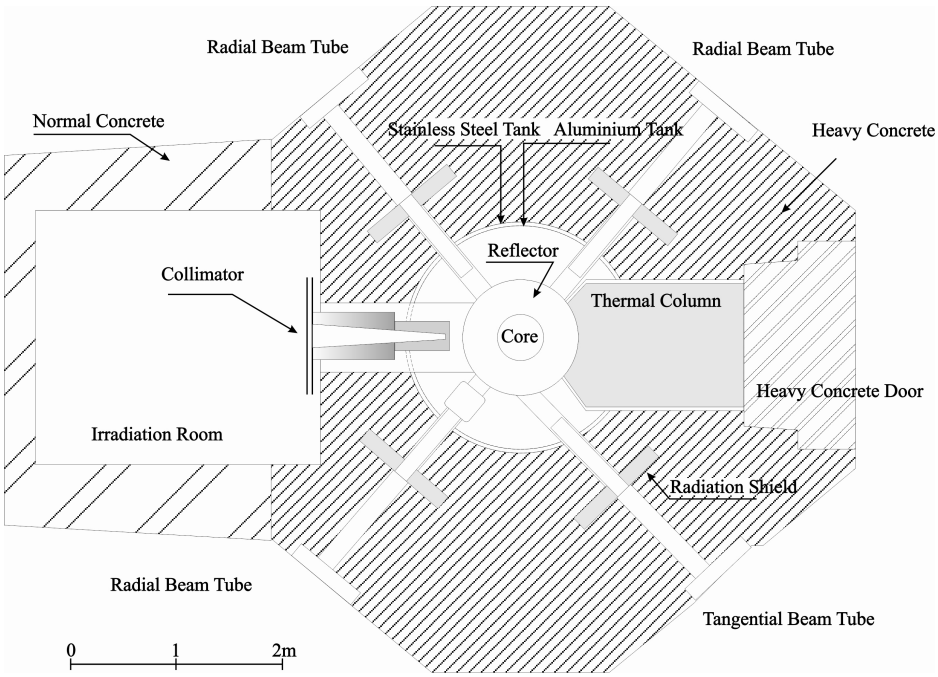

Figure 2.3.3: Horizontal section of the TRIGA Mark II Reactor in Vienna [14]

Chapter 3

Serpent - a Reactor Physics Code

The Serpent code is a Monte Carlo based reactor physics code. It has been in development since 2004 at VTT Technical Research Centre of Finland. The working title was "Probabilistic Scattering Game" or PSG. In October 2008 the name was changed to Serpent. Since 2009 Serpent 1 is available at OECD/NEA Data Bank and RSICC. In 2010 it was decided to rewrite the code and Serpent 2 was developed, currently Serpent 2 is in the Beta-Testing Phase and is constantly evolving [2; 22].

3.1 Functionality of the Serpent Code

Serpent is a continuous-energy stochastic transport code for burn up calculations.
To define a three-dimensional geometric model of fuel element or a nuclear reactors, Serpent uses a universe-based combinatorial solid geometry (CSG), likewise to MCNP and other reactor physics code. The geometry is built up of material cells, which are defined by diverse surface types. With this most of the reactor geometry can be modelled. In the code some additional geometry features are included, to simplify the definition of cylindrical fuel pins and different core layouts [2].

The simulation can run in two modes, the k-eigenvalue criticality source or with an external source. In the first method the first cycle starts at $k_{eff} = 1$ and approaches the right value after each cycle, in the external source mode all starting neutrons are emitted by an user-defined source.

The calculation of the neutron transport is based on a combination of two methods. The surface-to-surface ray-tracing and the Woodcock-delta-tracking method [2].

The conventional *surface-to-surface* ray-tracing tracks each neutron until it collides or reaches a material boundary. Then it recalculates the distance to the next boundary, and the process is repeated.

Serpent also uses the *Woodcock-delta-tracking method*, this method samples the next collision point without handling the surface crossing. It is based on virtual collision, also named as pseudo-scattering reaction. In the case of a virtual collision the neutron is not absorbed and the incident energy and the direction of flight are preserved. This interaction is characterised by the cross section $\Sigma_0(\mathbf{r}, E)$ given by:

$$\Sigma_0(\mathbf{r}, E) = \Sigma_m(E) - \Sigma_t(\mathbf{r}, t) \tag{3.1}$$

Σ_t is the total physical cross section of the material and Σ_m is the majorant cross section, the maximum of all total cross sections in the system. Σ_m is the same for all materials. The probability of sampling a virtual collision is the virtual cross section over the majorant cross section:

$$P = \frac{\Sigma_0}{\Sigma_m} \tag{3.2}$$

The free path length is sampled by using the majorant cross section. Then the collision of the neutron is sampled, either virtual or real. The virtual collision does not affect the state of the neutron, so this procedure is repeated until a real collision is sampled. This method is independent of whether different materials are crossed by the neutron [12].

This combination of methods is efficient in reactor geometries with fuel assemblies. But the delta-tracking method is not good for small or thin volumes which are far away or isolated from the active source, because it cannot estimate the track-length of the neutron flux. The latter has to be calculated in a less efficient manner by a collision estimator [2].

The sequence of the individual steps of the Serpent code in κ-eigenvalue criticality source mode are shown the following flow chart 3.1.1:

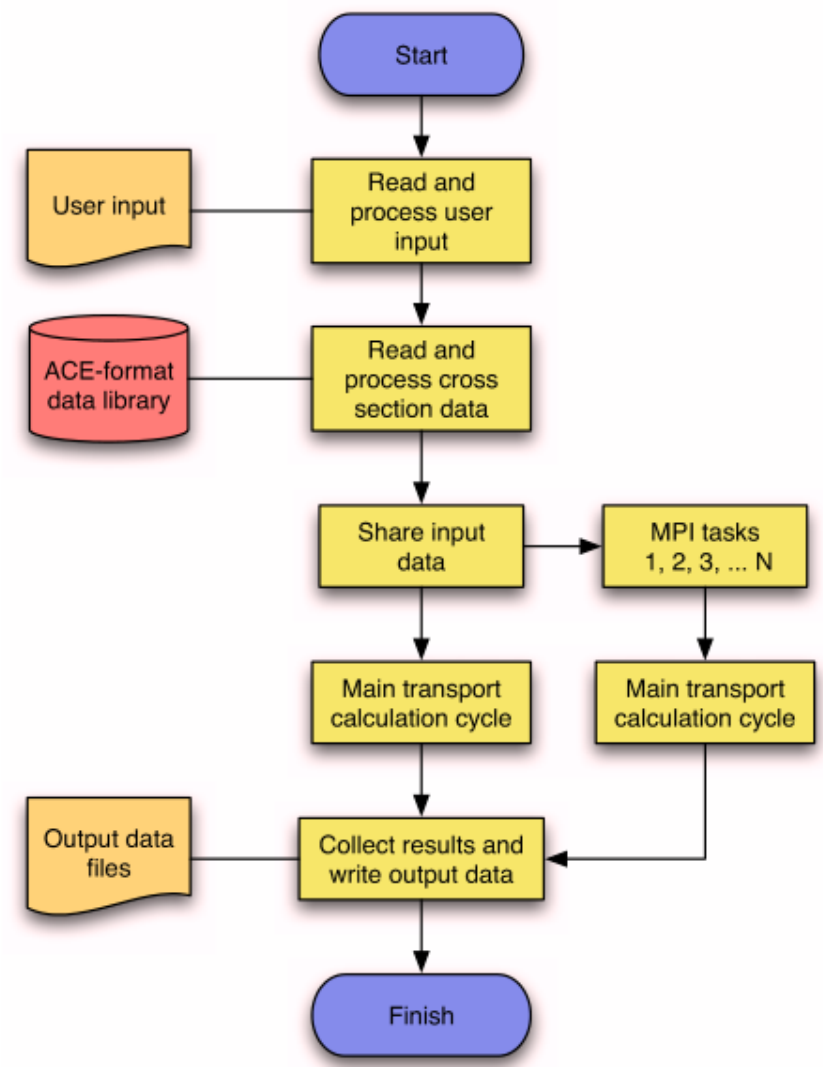

Figure 3.1.1: Flow chart of the transport cycle of Serpent in κ-eigenvalue criticality source mode [12]

The neutron account for the source distribution in the next cycle is given by the fission neutrons.

The user input defines the geometry, the materials and the options for the calculation routine. It also defines which data library should be used. After transport calculation Serpent can run a burn up calculation, this one is described in section 3.3.
Serpent can run calculations in parallel. In Serpent 2 parallelization is based on a hybrid OpenMP/ MPI approach [2]. The number of parallel tasks is based on CPU cores of the used computer [23].

3.2 Data Base

The physics of neutron interaction are based on classical collision kinematics. Cross sections, reaction laws and probabilities are collected in a nuclear data base. Serpent receives the information about continuous energy cross section from data libraries in ACE format. In the Serpent installation package the following libraries are included: JEF-2.2, JEFF-3.1, JEFF-3.11, ENDF/B-VI.8 and ENDFB/B-VII. These contain cross sections data for 432 nuclides at six different temperatures (300 K, 600 K, 900 K, 1200 K, 1500 K and 1800 K). Also radioactive decay and fission yield data are available in those libraries for over 4000 nuclides and meta-stable states.
Serpent does not use the continuous energy cross section directly from the libraries but first reconstructs a master energy grid and then starts the neutron transportation simulation. The macroscopic cross section for every material is also calculated before the transport simulation starts. The advantage of this procedure is the time saved during the transportation calculation [23].
To get more temperature-sensitive applications, a Doppler-broadening preprocessor routine is built in, this allows a conversion of ACE format crossing into higher temperatures [2].

3.3 Burn Up Calculation

For simple geometries such as a cylinder or a cube Serpent can calculate the volume and masses automatically from the surface and material cards. The reaction rates are normalized to total power, specific power density, flux or fission rate.
The user defines the burnable material and Serpent selects fission products and actinide daughter nuclides automatically. Burnable materials can be sub-divided into several depletion zones. A fuel element can for example be divided along the z-axis, therefore the outputs for burned material are also divided into smaller areas along the z-axis, instead of being for the total area.
The burn up calculation itself is based on built in calculation routines, without any external coupling. There are two options to solve the Bateman depletion equation [22]:

- Transmutation Trajectory Analysis (TTA): It is an analytical solution of linearized depletion chains.

- Chebyshew Rational Approximation Method (CRAM): An advanced matrix exponential solution for Serpent developed at the VTT in Finland

The irradiation history can be set by burn up time (in days) or cumulative burn up given in MWd/kgU. If several interval steps are needed, the normalization of the reaction rate can be changed in every step [23]. Serpent used a spectrum collapse method to speed up the calculation, meaning that the integral one-group transmutation cross sections are calculated within the transport cycle or the continuous-energy cross sections are collapsing after the cycle by using the flux spectrum [2].

3.3.1 Burn Up Outputs

The output of a burn up are given material-wise and in total values for parameters like isotopic composition, activities, spontaneous fission rates and decay heat data. These parameters are printed after each burn up step. Additionally the composition of the burned material can be printed out [2].

Part II

Simulation

Chapter 4

Development and Validation of the Serpent Model of TRIGA Mark II Vienna

The present chapter describes the implementation of a new model for the TRIGA Mark II reactor of the Technical University of Vienna by means of Serpent. Decision taken for the development of the geometry, the utilization of material cards and other option are here discussed.
Then the validation of the new Serpent model is described, by comparison of calculated neutron Flux and neutron energy spectrum with other available data, both experimental and calculated with the reactor MCNP model.

4.1 Serpent Reactor Model

4.1.1 Geometry Input

The three-dimensional model of the reactor was developed in Serpent. A top view of the reactor with the core configuration, of the year 2015 is shown in picture 4.1.1. The origin of the Serpent geometry is in the middle of the core.
The detailed geometry and material information was taken from an MCNP model. This model contains all essential core components described in section 2.2. The same simplifications were done at the fuel elements, the aluminium fixture at the bottom and the top of every FE were not modelled, but this will have no significant effect on the neutron transportation calculation inside the core. Furthermore, the thermal column was not modelled because the

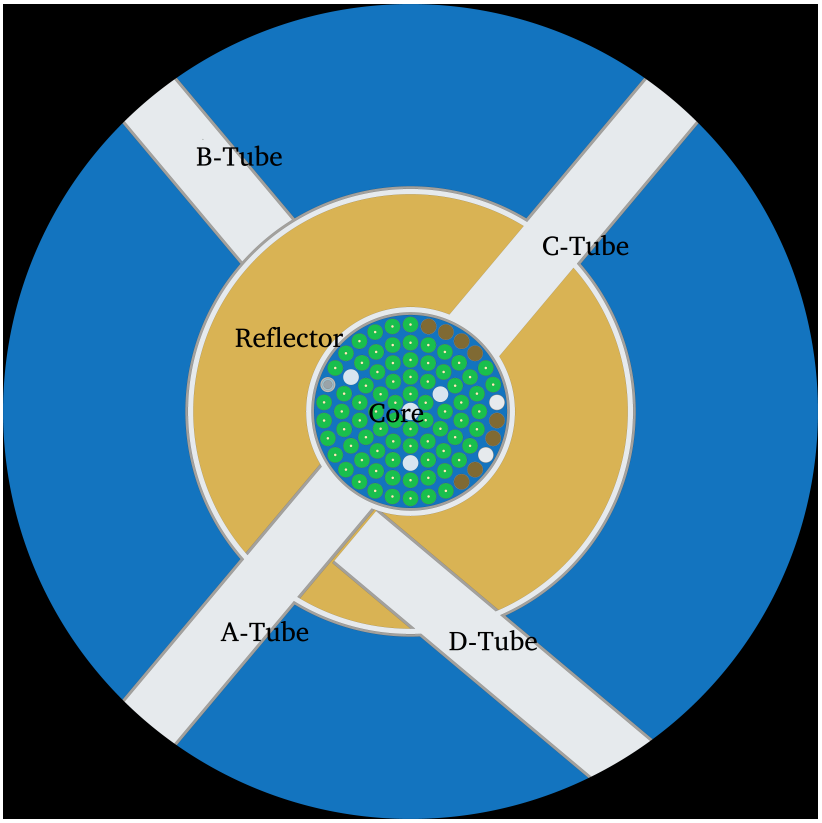

Figure 4.1.1: xy-plot of the Serpent core model at z = -9.65 cm (below the middle of the core)

effect, manifests itself only in the border regions of the reactor and will therefore have no significant effect on the following problems. Figure 4.1.2 is a vertical cross section of the model.
The colours in the plot represent different materials. Descriptions of all materials can be found in section 4.1.2. In figure 4.1.2 the structure of a FE is shown in more detail. The figure is a cross section of the FE, the cylindrical Zr-rod is surrounded by the Fuel meat (green). At the top and the bottom of the FE are graphite reflectors. At the lower part of the FE a Molybdenum-disk is placed.

The control rods were not modelled because the simulation is always running at full power (250 kW) where the control rods are in *up* position, so above the core. The model shows water at the position where the control rods are usually placed.
In the model the core is placed in a cylindrical water tank, with a radius of 100 cm and total hight of 120 cm. Also the beam tubes and the annular groove graphite reflector are modelled, see figure 4.1.1.

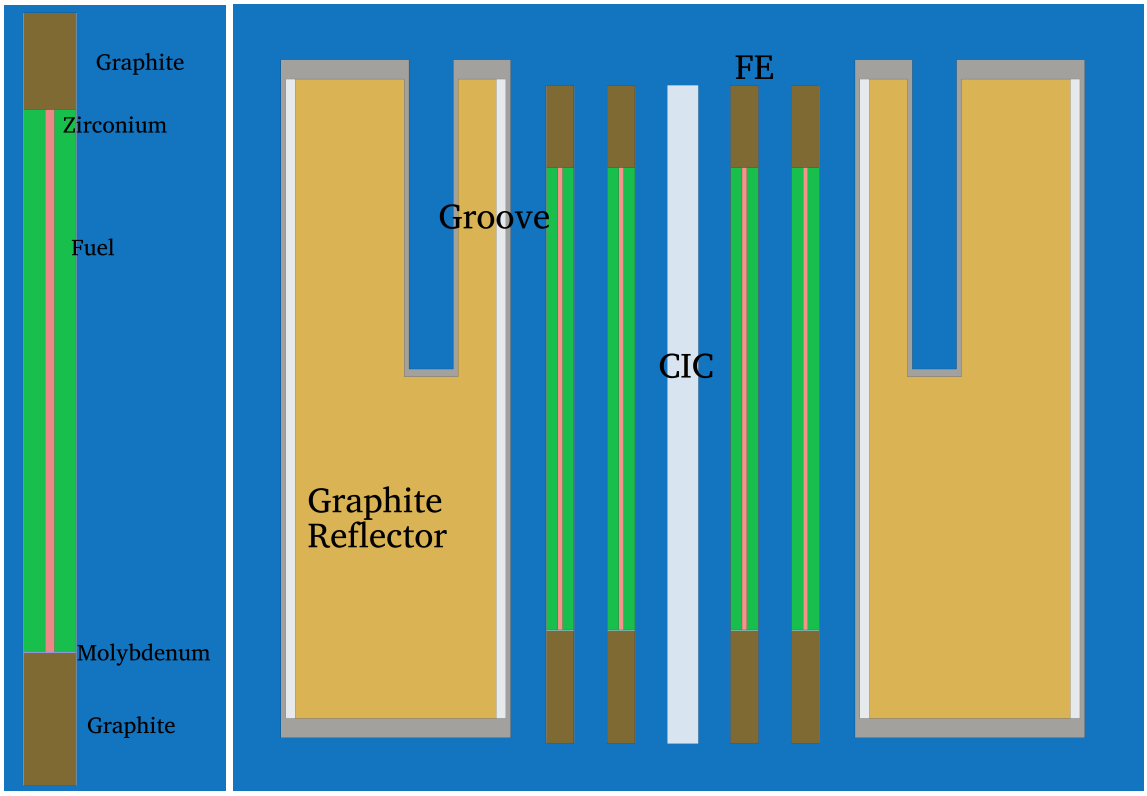

(a) zx-plot of Serpent fuel element

(b) zx-plot of the Serpent core model

Figure 4.1.2: zx-plots of Serpent fuel element (a) and plot of the core at y= 0 cm (b)

4.1.1.1 Surface Cards

The surface cards define the borders of the cells. Surface cards have a specific geometry. Those most often used in the input were: sphere, cylinder and plane surfaces. The syntax to define a surface in Serpent is:

```
surf <id> <type> <para1> <para2> ...
```

id is the identifying number set by the user, *type* is the type of the surface, such as a sphere or a plane. This is followed by a list of the parameters. For example for a sphere it is the origin (x, y, z) and the radius [23].
Some examples of the input file are shown in table 4.1.1.1.

Surface Input	Explanation
`surf 2 cyl 0.0 0.0 1.815`	Cylinder parallel to z-Axis (cyl), origin in x=0 and y=0 with the radius r=1.815 cm, it is the cylinder for the fuel meat
`surf 12 pz 19.05`	plane perpendicular to z-Axis (pz) at z=19.05 cm, it is the upper end of the fuel meat in a fuel element
`surf 2000 sph 0.0 0.0 0.0 0.6`	sphere (sph) at the origin x=y=z= 0 and with a radius of r=0.6 cm

Table 4.1.1: Same surface examples of the input file

Surface cards are needed to define the border of the cells.

4.1.1.2 Cell Cards

Cell cards define cells, each cell is filled with a material, the borders are bound by surfaces. The Serpent syntax looks as followes:

```
cell <id> <uni> <mat> <surf1> <surf2> ...
```

id is again a number to identify the cell, *uni* is the universe number and *mat* is the name of the material in the cell, this is followed by a list of surfaces. [23] One example of my input file is:

```
cell 1011 10 fuel 1 -2 13 -12
```

It is the cell 1011 in the universe 10, the material is fuel, and the surfaces 1 and 2 are cylindrical surfaces parallel to the z-axis, the surfaces 13 and 12 are planes perpendicular to the z-axis. This cell 1011 also defines the material between the first and the second cylinder the upper and lower boundaries are set by the two planes. The radius of cylinder 1 is the radius of the Zr-rod inside the fuel element. The radius of cylinder 2 is the radius of the fuel element. The cell 1011 is also the fuel cylinder where the Zr-rod is cut out.
Serpent uses different universes to nest parts into each other. The universes are identified by a user-defined number, the most outer universe should have the number 0.

The following paragraphs explain the structure of the geometry input of the TRIGA reactor in Vienna, starting from the beginning with the inner parts and moving outwards.

4.1.1.3 Universes and structure of the input file

The core elements were modelled separately and placed afterwards in the right position. The fuel cylinder was modelled with the origin at x=0 cm, y=0 cm and then placed in a lattice. This was done the same way for every core element, such as control rods, dummy graphite elements, the neutron source and irradiation tubes. Every element has its own universe number, for example the fuel elements have the universe number 10 and the dummy graphite elements have the number 11. This universe number is used to arrange them in the annular core lattice.
The core of the TRIGA reactor Vienna has a circular cluster array. Serpent has a predefined lattice for this type of array amongst other. This predefine lattice structure has to filled by regular structure of other universes, like the fuel pins and dummy graphite elements. The syntax for the TRIGA reactor core is:

```
lat 100 4 0 0 6
```

lat is the command, that a predefined structure is to follow, *100* is the universe number of the lattice (thus the universe of the reactor core), *4* is the lattice type, a circular cluster array where *0 0* are the origin coordinates (x,y) and 6 are the number of rings. This column is followed by a list of rings. The rings are defined by:

```
<n> <r> <theta> <u1> <u2> ...  <un>
```

n is the number of elements in the ring, *r* is the radius of the ring, *theta* is the angle of rotation and *u* is the number of the universe filling this ring. In the case if the TRIGA reactor the inners ring (A-ring) has 1 element and the next ring (B-ring) 6 elements and so on, this is number *n*. The radius of the A-ring is 0 cm and 4.15 cm for the B-ring. To arranged the core in Serpent the same way as in MCNP, and in the core in figure 2.2.2 the rings are rotated by 30°. The universes number are the from the cell cards of the fuel elements and dummy graphite elements, etc. [23].
Between the core elements and around the core water is placed.
The inner parts of the geometry model is now placed. The core universe 100 is filled by the

core components with their own universe numbers.

Furthermore the reflector is designed separately. In figure 4.1.2 a vertical section of the reflector is shown. The Graphite reflector is cladded with aluminium, between the cladding and the graphite is an air gap. Also in the reflector the annular grooved for irradiation experiments is placed. To avoid any geometry errors by Serpent (for example through overlapping cells) the reflector is divided into four parts, each with their own universe number. The first part is from the core site of the reflector to the annular groove (u=201). The second is the annular groove (u=202), the third is the part of the reflector right under the groove (u=203) and the fourth is the outer part of the reflector (u=204). This division is shown in figure 4.1.3.

The four beam tubes and the water tank are shown in figure 4.1.1, passing through the reflector. The tubes were modelled separately and the reflector universe is then filled by the tubes.

The core, and the reflector with the tubes are then placed in the water tank. The water tank is the outermost universe so it has the number 0. It is filled by the core and the four parts of the reflector, plus the parts of the beam tubes in the water tank (see figure 4.1.1). The shape of the tank is cylindrical and the dimensions of the water tank in the Serpent model are:

- **total height**: 1.2 m
  - 0.6 m above the core centre
  - 0.6 m below the core centre
- **Radius of the tank cylinder**: 0.965 m

In reality the tank is bigger, but these dimensions are sufficient for the studied issues to the simulation. The material of the cell beyond the tank is "`outside`", this

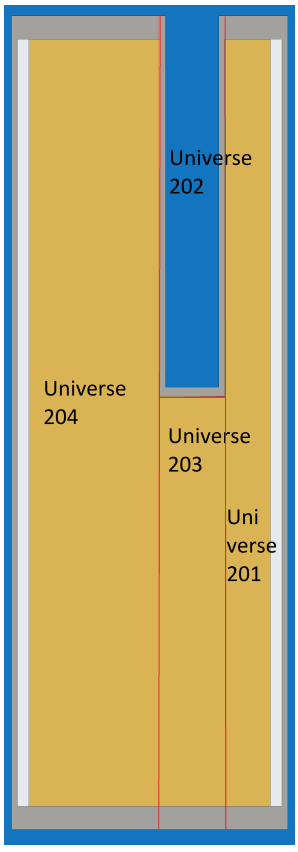

Figure 4.1.3: Detail of the Graphite Reflector, for the Serpent Simulation the reflector is divided into four universes, the red lines are their boundaries

means, that the boundaries for the Serpent
calculations are set to the tank extension.

4.1.2 Material Cards

The neutron reaction data which Serpent uses for transportation calculation are taken from the OECD/NEA Data Bank. Serpent provides libraries based on JEF-2.2, JEFF-3.1, ENDF/B-VI.8 and ENDF/B-VII. For the following simulation the ENDF/B-VII library was used.

The user defines the material specification in the input file in Serpent in the form of a material card. Each material has its own card. The card defines the name of the material and the density (mass or atomic), followed by a list of the nuclides that constitute the material with the corresponding fraction (in mass or atomic) [23].
The materials which were used for the Serpent input, are for the fuel as follows:

Nuclide	**Mass Fraction**
U-235	0,0166
U-238	0,0667
Zr-90	0,9012
H-1	0,0155

Table 4.1.2: Composition of the fuel meat

This composition corresponds to a fresh fuel element.
The Zirconium rod and the Molybdenum disk in the fuel element have the composition of natural Zirconium and natural Molybdenum.

The fuel element is cladded with stainless steel (SS) type 304, the composition of this material is shown in table 4.1.3.

Graphite is used as a reflector at the top and the bottom of each fuel element, as well as in the core surrounding reflector. The material entry is natural graphite with a mass density of 1 g/cm^3.

The aluminium cladding of the reflector is Al-27 with a mass densities of 1 g/cm^3.

Nuclide	Mass Fraction
Fe-54	0,0397
Fe-56	0,6226
Fe-57	0,0144
Fe-58	0,0019
Cr-50	0,0078
Cr-52	0,1508
Cr-53	0,0171
Cr-54	0,0043
Ni-58	0,0686
Ni-60	0,0294
Mn-55	0,018
Si-28	0,01
P-31	0,0045
S-32	0,003
C-nat.	0,008

Table 4.1.3: Composition of the SS-cladding type 304

For the neutron source Antimony (Se-21 with 57,21% and Se-23 with 42,79% natural abundance) and Beryllium (Be-9) were used.

Otherwise, water and air were needed to complete the reactor.

A thermal scattering card provides correct reactions data for moderator materials. This is important because otherwise thermal systems ware modleled by using free-atom criss section and this will introduced significant errors. [23] To avoid this for this materials like water, graphite and Zirconium-Hydrogen thermal scattering cards are set, which takes the thermal properties into account. This cards were taken from the MCNP 6 libraries and transfers to the Serpent libraries. Because Serpent doesn't provide thermal scattering for Zirconium-Hydrogen, but in the TRIGA fuel Zirconium-Hydrogen is a main component and can not be neglected.

4.2 General Options and Parameters of the Serpent Calculation

The simulation is run with 1 million source neutron in 1500 cycles, where the first 70 cycles are skipped. The model starts with the initial guess of $k_{eff} = 1$ and after 70 cycles the k_{eff} value has an accepted value.
The unresolved resonance probability tables are switched on.

The main output file from the Serpent simulation consists of many values and parameters. First, the file lists the technical parameters under which the simulation runs and the user-defined options. In addition, it contains all the results of the calculation, such as criticality eigenvalues, radioactivity data, Normalisation coefficient and the normalized total reaction rates, Forward-weighted delayed neutron parameters and some more. The criticality eigenvalue k_{eff} of the TRIGA Serpent core Model is:

$$\boxed{k_{eff} = \quad 1.02583 \pm 3.2 \times 19^{-5}}$$

4.3 Neutron Flux Calculation in the Reactor Core

The first step to validate the Serpent model is to detected the neutron flux at different position and compare the results with the verified data of the Monte Carlo code MCNP6 published in [24].

A visualisation of the thermal flux can be seen in figure 4.3.4. This mesh plot is an graphic file created by Serpent. Shades of red and yellow represents the relative fission power and shades of blue and white representing the relative thermal flux (below 0.65 eV) [23]. This figure 4.3.4 is just a quantitative visualisation of the thermal flux.
The neutron flux was simulated at four different positions along the radial direction, and at 11 positions along the z-axis in the Central Irradiation Tube (CIT). The position in the radial direction are in the CIT and the irradiation position *b*, *i* and *o* in figure 2.2.2. The distances are reported in table 4.3.4,

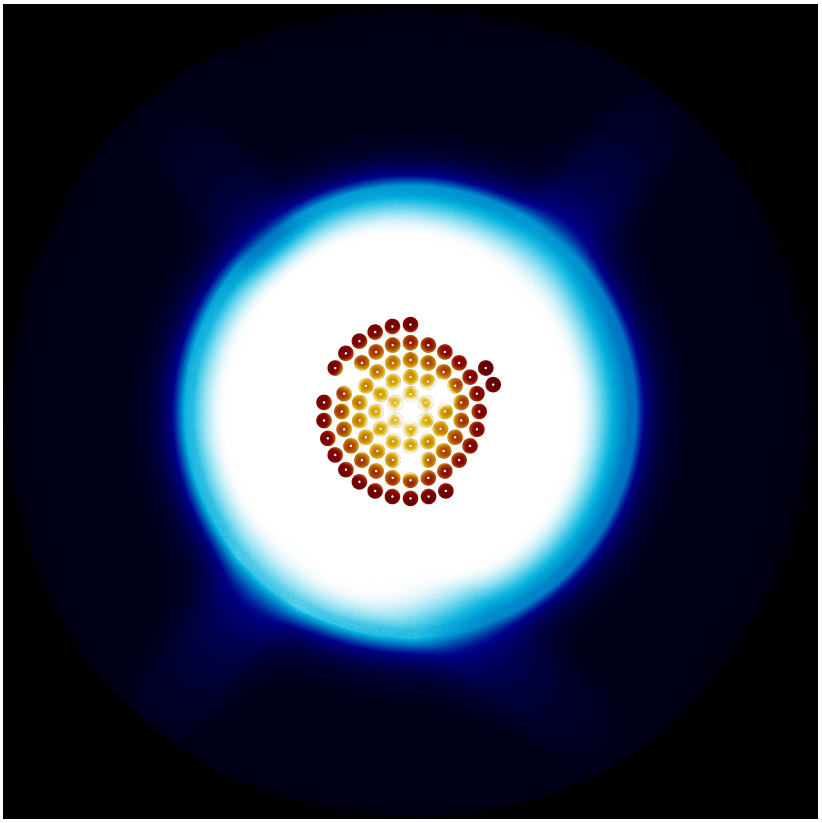

Figure 4.3.4: Mesh plot of the relative thermal flux (blue and white shades) and relative fission power (red and yellow shades) created by the Serpent program at z = 0 cm

Position	**Radial distance along x-axis** [cm]
6	0
b	-5.0
i	-13.5
o	-22.0

Table 4.3.4: Radial Irradiation Position

Position	**Vertical distance along z-axis** [cm]
1	20
2	16
3	12
4	8
5	4
6	0
7	-4
8	-8
9	-12
10	-16
11	-20

Table 4.3.5: Vertical Irradiation Position in the CIT

In radial direction the positions are in equatorial level of the core (z=0 cm) and Position 6 correspond to the core centre.

At the position of interest, a detector was placed. For this, a detector of type cell detector was selected. These are calculated in a cell using collision estimate of neutron flux, the differential flux is provided in the output file [23].
he power of the reactor was kept 250 kW.
The detector cell was a sphere filled with water with a radius of 0.6 cm.
In the output the differential flux for every position is provided for 30 energy groups between 0 and 18 MeV. The width of these energy groups has been chosen to represent constant lethargy intervals as in precious MCNP calculation. Multiplying by the bin width, the integral flux can be calculated.

4.3.1 Flux in the Radial Direction

The differential flux spectra from MCNP and Serpent are compared in figure 4.3.5.

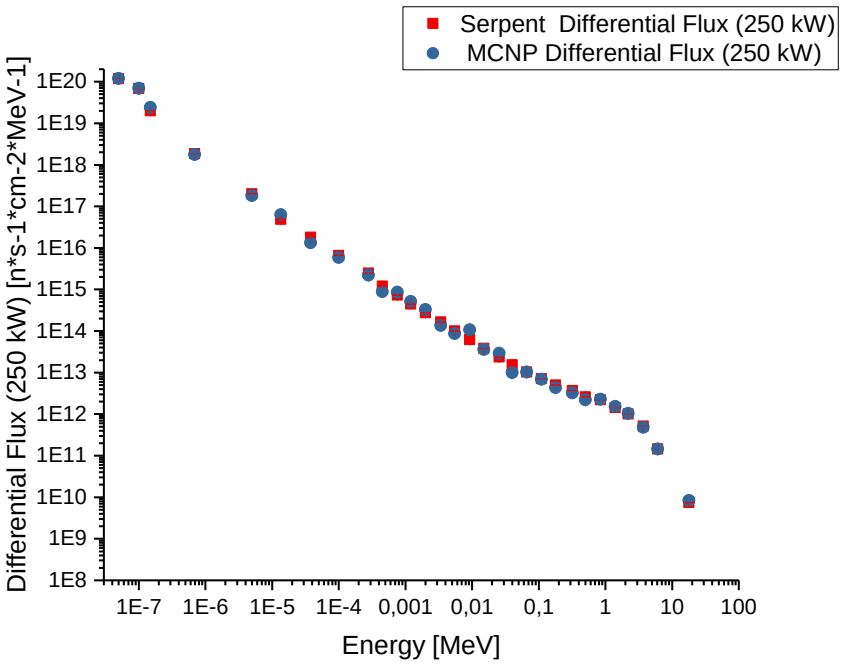

Figure 4.3.5: Differential Flux in Central Irradiation Tube Position 6 (Core Center)

By multiplying the differential flux with the width of the energy interval, one gets the integral flux. Figure 4.3.6 shows the thermal flux ($0 - 6,9 \times 10^{-7}$ MeV) and the total flux (0-18

MeV) comparison between Serpent and MCNP.

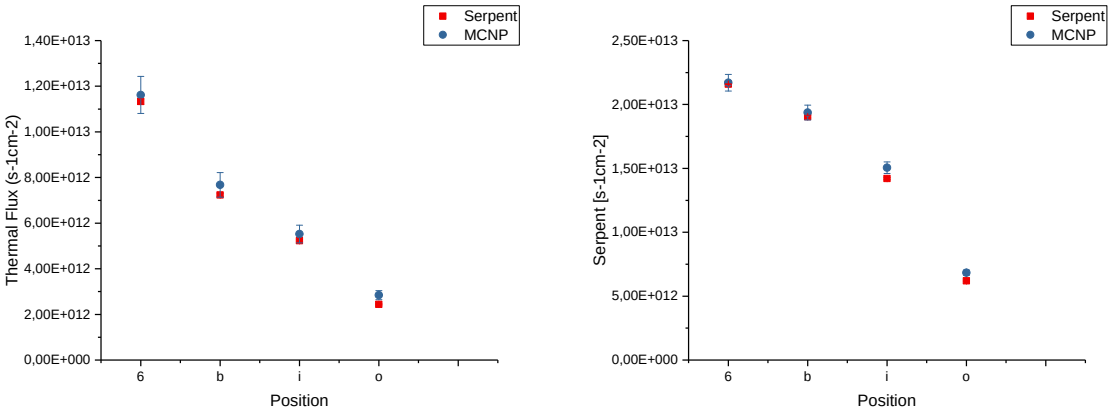

(a) Thermal neutron fluxes along the radial core direction obtain by Serpent and MCNP

(b) total neutron fluxes along the radial core direction obtain by Serpent and MCNP

Figure 4.3.6: Behaviour of the neutron flux in the radial direction

The statistic error in Serpent was 1% or lower, so the error-bars of the values from the Serpent calculation are not clearly visible. The error of the MCNP simulation was 7% for thermal flux and 3% for total flux.

After comparing MCNP and Serpent, it can be stated that they are in very good agreement. The difference are mostly below 10%, just in position *o* the differences between the two simulations is 14 %.

It has been shown that the further away from the center the neutron flux is represented, the greater the difference between Serpent and MCNP.

The obtained values from Serpent for the neutron flux in radial direction can be found in table 4.3.1.

Radial Position	**Thermal Flux** [$s^{-1}cm^{-2}$]	**Total Flux** [$s^{-1}cm^{-2}$]
6	$1.13{\cdot}10^{13} \pm 1.13{\cdot}10^{11}$	$2.16{\cdot}10^{13} \pm 2.68{\cdot}10^{10}$
b	$7.24{\cdot}10^{12} \pm 7.24{\cdot}10^{10}$	$1.91{\cdot}10^{13} \pm 1.02{\cdot}10^{11}$
i	$5.23{\cdot}10^{12} \pm 5.23{\cdot}10^{10}$	$1.42{\cdot}10^{13} \pm 8.84{\cdot}10^{10}$
o	$2.44{\cdot}10^{12} \pm 2.44{\cdot}10^{10}$	$6.20{\cdot}10^{12} \pm 5.71{\cdot}10^{10}$

Table 4.3.6: Neutron Flux in radial direction obtained by Serpent

4.3.2 Fluxes in the Vertical Direction

In the Serpent model the Central Irradiation Tube was filled with water, and along the z-axis 11 cell-detectors, in sphere shapes, were placed, each with a radius of 0.6 cm. The integral fluxes are shown in the figure 4.3.7:

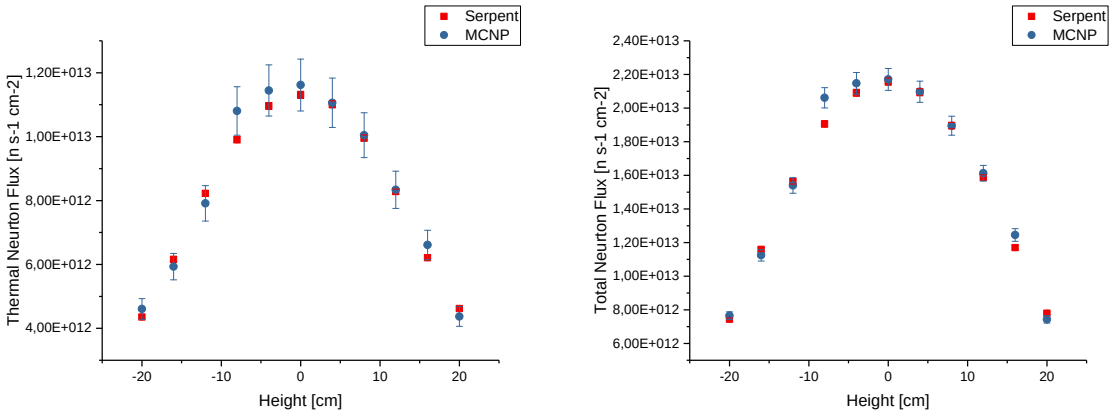

(a) Thermal neutron fluxes along the z-axis in CIT obtained by Serpent

(b) Total neutron fluxes along the z-axis in CIT obtained by Serpent

Figure 4.3.7: Behaviour of the neutron flux in the vertical direction in CIT

The statistical error of the Serpent simulation is less than 1%.

Vertical Position [cm]	**Thermal Flux** [$s^{-1}cm^{-2}$]	**Total Flux** [$s^{-1}cm^{-2}$]
20	$4.62 \cdot 10^{12} \pm 4.62 \cdot 10^{10}$	$7.79 \cdot 10^{12} \pm 7.79 \cdot 10^{10}$
16	$6.21 \cdot 10^{12} \pm 6.21 \cdot 10^{10}$	$1.17 \cdot 10^{13} \pm 1.17 \cdot 10^{11}$
12	$8.28 \cdot 10^{12} \pm 8.28 \cdot 10^{10}$	$1.59 \cdot 10^{13} \pm 1.58 \cdot 10^{11}$
8	$9.96 \cdot 10^{12} \pm 9.96 \cdot 10^{10}$	$1.90 \cdot 10^{13} \pm 1.90 \cdot 10^{11}$
4	$1.10 \cdot 10^{13} \pm 1.10 \cdot 10^{11}$	$2.09 \cdot 10^{13} \pm 2.09 \cdot 10^{11}$
0	$1.13 \cdot 10^{13} \pm 1.13 \cdot 10^{11}$	$2.16 \cdot 10^{13} \pm 2.16 \cdot 10^{11}$
-4	$1.10 \cdot 10^{13} \pm 1.10 \cdot 10^{11}$	$2.09 \cdot 10^{13} \pm 2.09 \cdot 10^{11}$
-8	$9.91 \cdot 10^{12} \pm 9.91 \cdot 10^{10}$	$1.91 \cdot 10^{13} \pm 1.89 \cdot 10^{11}$
-12	$8.22 \cdot 10^{12} \pm 8.22 \cdot 10^{10}$	$1.56 \cdot 10^{13} \pm 1.56 \cdot 10^{11}$
-16	$6.16 \cdot 10^{12} \pm 6.16 \cdot 10^{10}$	$1.16 \cdot 10^{13} \pm 1.16 \cdot 10^{11}$
-20	$4.35 \cdot 10^{12} \pm 4.35 \cdot 10^{10}$	$7.44 \cdot 10^{12} \pm 7.44 \cdot 10^{10}$

Table 4.3.7: Neutron Flux in vertical direction obtained by Serpent

4.4 Fluxes in Fuel Element

For burn up calculation the behaviour of the neutron fluxes inside a fuel element is of interest. Because of this the neutron flux inside a fuel element was compared, from the Serpent simulation and the verified MCNP model.
The analysed fuel element was the FE 9213 in Position B2.
The fuel meat was divided into nine parts along the z-axis, each of these cells was a detector for the neutron flux. The top and the bottom cell were 4.5 cm high and the other cells 4.2 cm. Otherwise, they had the same characteristics as a fuel element, excluding the central Zr-rod.

The obtained total and thermal fluxes are shown in figure 4.4.8 and table 4.4:

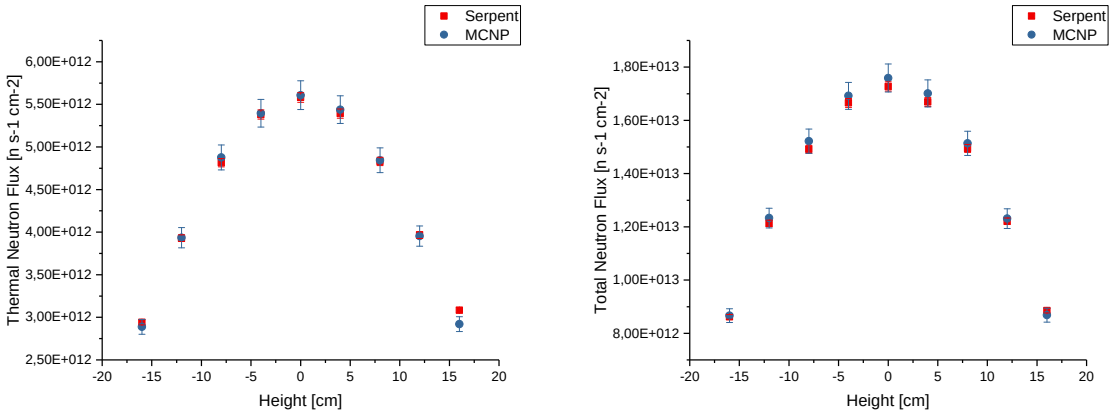

(a) Thermal neutron fluxes in FE obtained by Serpent and MCNP

(b) Total neutron fluxes in FE obtained by Serpent and MCNP

Figure 4.4.8: Behaviour of the neutron flux inside fuel element B2-9213

The statistical error is less than 1% in the Serpent simulation and less than 3 % in the MCNP. The difference between the MCNP model and the Serpent model is insignificant, the highest is 5%.
From this it was concluded that Serpent represents the neutron flux very well inside a fuel element.

The further one goes outwards, the neutron flux decreases. This was verified by calculating the neutron flux with Serpent in various fuel elements as from ring B to E. The neutron flux in this different fuel elements can be seen in the figure 4.4.9 and the values can be found in

table 4.4 and table 4.4.

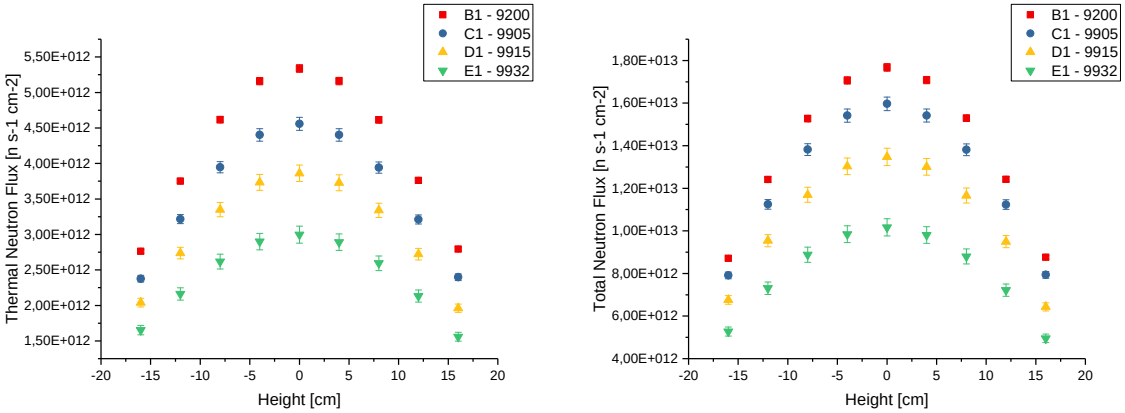

(a) Thermal neutron fluxes in different Fuel Elements obtained by Serpent

(b) Total neutron fluxes in different Fuel Elements obtained by Serpent

Figure 4.4.9: Behaviour of the neutron flux in different Fuel Elements

For the fuel elements in the B-ring an uncertainty of 1 % was assumed, for the C-ring 2%, 3% for the D-ring and 4 % for the E-ring. Because the comparison of the Serpent and the MCNP Simulation of the neutron flux in the radial direction has shown that the consistency decreases towards the outside.

Height [cm]	**B2-9213**	**B4-9214**	**C1-9905**	**D1-9915**	**E1-9932**
16	$3.08{\cdot}10^{12}$	$2.79{\cdot}10^{12}$	$2.40{\cdot}10^{12}$	$1.96{\cdot}10^{12}$	$1.56{\cdot}10^{12}$
12	$3.97{\cdot}10^{12}$	$3.76{\cdot}10^{12}$	$3.21{\cdot}10^{12}$	$2.72{\cdot}10^{12}$	$2.13{\cdot}10^{12}$
8	$4.83{\cdot}10^{12}$	$4.61{\cdot}10^{12}$	$3.94{\cdot}10^{12}$	$3.34{\cdot}10^{12}$	$2.59{\cdot}10^{12}$
4	$5.39{\cdot}10^{12}$	$5.16{\cdot}10^{12}$	$4.40{\cdot}10^{12}$	$3.73{\cdot}10^{12}$	$2.89{\cdot}10^{12}$
0	$5.58{\cdot}10^{12}$	$5.34{\cdot}10^{12}$	$4.56{\cdot}10^{12}$	$3.86{\cdot}10^{12}$	$3.00{\cdot}10^{12}$
-4	$5.38{\cdot}10^{12}$	$5.16{\cdot}10^{12}$	$4.40{\cdot}10^{12}$	$3.73{\cdot}10^{12}$	$2.90{\cdot}10^{12}$
-8	$4.82{\cdot}10^{12}$	$4.62{\cdot}10^{12}$	$3.95{\cdot}10^{12}$	$3.35{\cdot}10^{12}$	$2.62{\cdot}10^{12}$
-12	$3.93{\cdot}10^{12}$	$3.75{\cdot}10^{12}$	$3.22{\cdot}10^{12}$	$2.74{\cdot}10^{12}$	$2.16{\cdot}10^{12}$
-16	$2.94{\cdot}10^{12}$	$2.76{\cdot}10^{12}$	$2.38{\cdot}10^{12}$	$2.04{\cdot}10^{12}$	$1.65{\cdot}10^{12}$

Table 4.4.8: Thermal Flux [$s^{-1}cm^{-2}$] in the different Fuel Elements along the z-axis

Height [cm]	**B2-9213**	**B4-9214**	**C1-9905**	**D1-9915**	**E1-9932**
16	$8.85{\cdot}10^{12}$	$8.76{\cdot}10^{12}$	$7.94{\cdot}10^{12}$	$6.43{\cdot}10^{12}$	$4.95{\cdot}10^{12}$
12	$1.22{\cdot}10^{13}$	$1.24{\cdot}10^{13}$	$1.12{\cdot}10^{13}$	$9.50{\cdot}10^{12}$	$7.22{\cdot}10^{12}$
8	$1.49{\cdot}10^{13}$	$1.53{\cdot}10^{13}$	$1.38{\cdot}10^{13}$	$1.17{\cdot}10^{13}$	$8.80{\cdot}10^{12}$
4	$1.67{\cdot}10^{13}$	$1.71{\cdot}10^{13}$	$1.54{\cdot}10^{13}$	$1.30{\cdot}10^{13}$	$9.81{\cdot}10^{12}$
0	$1.73{\cdot}10^{13}$	$1.77{\cdot}10^{13}$	$1.60{\cdot}10^{13}$	$1.35{\cdot}10^{13}$	$1.02{\cdot}10^{13}$
-4	$1.67{\cdot}10^{13}$	$1.71{\cdot}10^{13}$	$1.54{\cdot}10^{13}$	$1.30{\cdot}10^{13}$	$9.84{\cdot}10^{12}$
-8	$1.49{\cdot}10^{13}$	$1.53{\cdot}10^{13}$	$1.38{\cdot}10^{13}$	$1.17{\cdot}10^{13}$	$8.88{\cdot}10^{12}$
-12	$1.21{\cdot}10^{13}$	$1.24{\cdot}10^{13}$	$1.12{\cdot}10^{13}$	$9.54{\cdot}10^{12}$	$7.31{\cdot}10^{12}$
-16	$8.62{\cdot}10^{12}$	$8.71{\cdot}10^{12}$	$7.91{\cdot}10^{12}$	$6.76{\cdot}10^{12}$	$5.27{\cdot}10^{12}$

Table 4.4.9: Total Flux [$s^{-1}cm^{-2}$] in the different Fuel Elements along the z-axis

4.5 Conclusion

Comparing the results from the neutron flux calculation from Serpent with data from previous MCNP calculation shows that the Serpent Core model is in a very good agreement with these data. In radial direction the difference between the two simulations is below 10 %. In the core centre the difference is the lowest with 2.5 % in the thermal flux and 0.5 % at the total flux.

The comparison of the neutron flux in vertical direction give also very good agreements, the difference here between the two simulation is below 8 %.

Inside the fuel element the difference between Serpent and MCNP is even lower, nearly everywhere below 3 %, just in the highest cell of the fuel element the difference between the two calculation is in the thermal flux 5 %, which is also a very good agreement.

These calculation shows that the Serpent model is a good tool to simulate the neutron flux in the reactor and can be used for further simulations.

Chapter 5

Irradiation of Uranium and Thorium Foil in the Reactor

This chapter describes the simulation of an experiment carried out at the TRIGA Mark II research reactor in Vienna in the year 2015 using the reactor model developed with Serpent-2. The experiment was an irradiation to obtain data about the production and depletion of nuclides in natural uranium (U-238) and thorium (Th-232) in the reactor. Thereby natural Uranium and Thorium foils were irradiated in the annular groove in the reflector.

5.1 Description of the Experiments

The samples for the experiment are natural Thorium and Uranium Foils, ordered by the company at "Goodfellow Cambrige Limited", the properties of the foils are the same as described in section 5.1.1. The foils were placed in a small polythene capsule which was then inserted in a irradiation capsule also made of polythene. This irradiation capsule was then inserted in a dry beam tube of the Lazy Susan (LS) irradiation channel. The irradiation position was LS 1 also shown in figure 2.2.2 and the coordinates are listed in section 5.1.1. The irradiation time of the foils was 90 minutes at a reactor power of 5 kW. The irradiation measurements were taken in February and March 2015 at the TRIGA reactor in Vienna. After irradiation, the samples were highly active and therefore they could not be removed immediately from the reactor core. They stayed in the core overnight (12 h) and the samples were removed the next morning. For good measurement results and safe handling a certain time between measurement and irradiation must have elapsed. The Gamma Spectroscopy of the probes was preformed with a gamma-detector from *Canberra*. The Measurements with the gamma-detector was done 11.13 days from the irradiation for the uranium sample

and 7.73 days from the irradiation for the Thorium foil. The measurement time was around 5000 seconds with a dead time of around 8 % [3].

5.1.1 Description of the Foils

Two different types of foil were investigated: The first set of foils were natural Uranium-foil and the second set natural Thorium-foil. The foils have a cylindrical shape. The specific characteristics of these foils, such as material and size, are listed in the table 5.1.1.

Material	**Composition** [ppm]
Uranium	99.97 %
Carbon	125
Chromium	20
Iron	125
Nickel	20
Silicon	20
Density [g/cm^3]	15.16
Radius [cm]	0.5
Height [μm]	1.78

Table 5.1.1: Properties of the Uranium Foil

Material	**Composition** [ppm]
Thorium	99.88 %
Aluminium	500
Boron	0.4
Cadmium	0.1
Calcium	250
Chlorine	8
Chromium	6
Copper	5
Iron	150
Lithium	0.1
Magnesium	10
Manganese	13
Nickel	5
Nitrogen	250
Silicon	10
Uranium	0.1
Density [g/cm^3]	11.724
Radius [cm]	0.5
Height [μm]	1.25

Table 5.1.2: Properties of the Thorium Foil

The coordinates of the LS1 position were:

$$x = -12\ cm, \quad y = -31\ cm, \quad z = 5.5\ cm$$

5.2 Serpent Simulation

To adjust the conditions of the real experiment in the Serpent Simulation, the foil was surrounded by an air and placed at the location LS1. The foil is placed in a irradiation tube filled with air. The diameter of the tube was 3.7 cm. Otherwise, the annular groove is filled with water. The simulated LS 1 position is shown in the following figure 5.2.1. The properties and the material composition was set like it is listed in table 5.1.1.

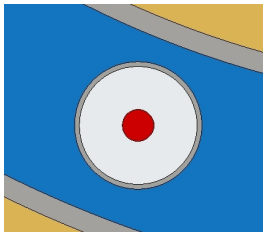

(a) enlarged xy cross section of the foil (red) with surrounding air (white)

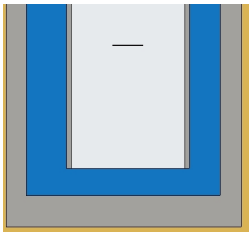

(b) enlarged view of the foil (xz)

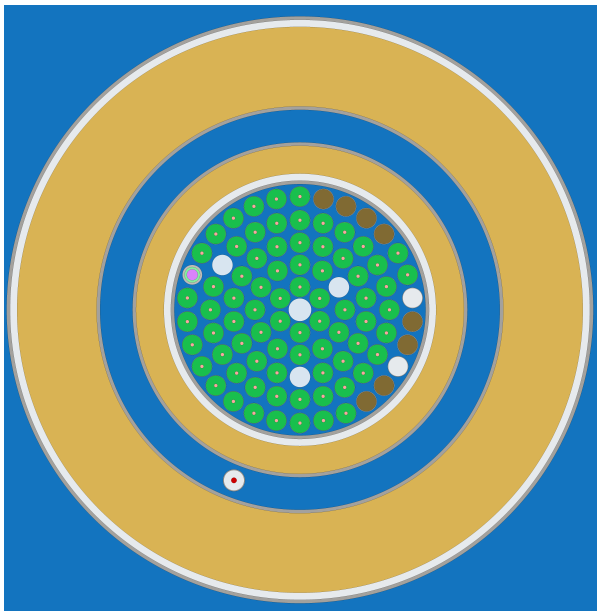

(c) Foil (red) with surrounding modelled by Serpent

Figure 5.2.1: The Position LS 1 with the foils (red)

The general simulation options were again 1 million source neutrons per cycles, in total 1500 cycles. To simulate the irradiation the burn up of the foils material was modelled by Serpent. The burn up time was 90 minutes and the power 5 kW.

5.3 Results of the Experiment and the Simulation

Measurements of the foil with γ-spectroscopy certain days after the irradiation shows activities of several isotopes. The isotopes which were found in the Uranium foils were: Ba-140, La-140, Mo-99, Tc-99m, Np-239, Ce-141, Nd-147, Te-132, I-132, I-131, Xe-133, Ce-143, Ru-103, Zr-95 and Nb-95. For the Thorium foil following isotopes were detected: Pa-233,

Th-232, Ba-140 and La-140.
Serpent can calculated activities of every possible isotope: to compare with measured data the output file consist the nuclide inventory list for the mention above isotopes and the total activity of the foil at the date of the measurements. These activities, which were calculated by Serpent, direct after the irradiation are listed below in tables 5.3.3 and 5.3.4. The uncertainty of the results of the Serpent simulation are approximately 10%.

Isotope	**Activity after Irradiation [Bq]**
Ba-140	$1.186 \cdot 10^4$
La-140	$2.246 \cdot 10^2$
Mo-99	$5.435 \cdot 10^4$
Tc-99m	$3.886 \cdot 10^3$
Np-239	$7.966 \cdot 10^5$
Ce-141	$3.158 \cdot 10^2$
Nd-147	$3.934 \cdot 10^3$
Te-132	$3.201 \cdot 10^4$
I-132	$8.591 \cdot 10^3$
I-131	$3.045 \cdot 10^3$
Xe-133	$3.763 \cdot 10^2$
Ce-143	$8.174 \cdot 10^4$
Ru-103	$1.877 \cdot 10^3$
Zr-95	$2.096 \cdot 10^3$
Nb-95	1.185
Total Activity	$2.789 \cdot 10^8$

Table 5.3.3: Activity of the Uranium Foil after 90 min of Irradiation at 5 kW as calculated by Serpent

The results for Thorium are in the table 5.3.4 below:

Isotope	**Activity after Irradiation**[Bq]
Pa-233	$7.383 \cdot 10^4$
Th-232	$4.664 \cdot 10^2$
Ba-140	22.948
La-140	0.292
Total Activity [Bq]	$6.520 \cdot 10^7$

Table 5.3.4: Activity of the Thorium Foil after 90 min of Irradiation at 5 kW calculated by Serpent

The determined activities of the uranium foil are shown in the following figure 5.3.2. Both the data determined by the Serpent simulation and the data determined with the aid of gamma spectroscopy are displayed.

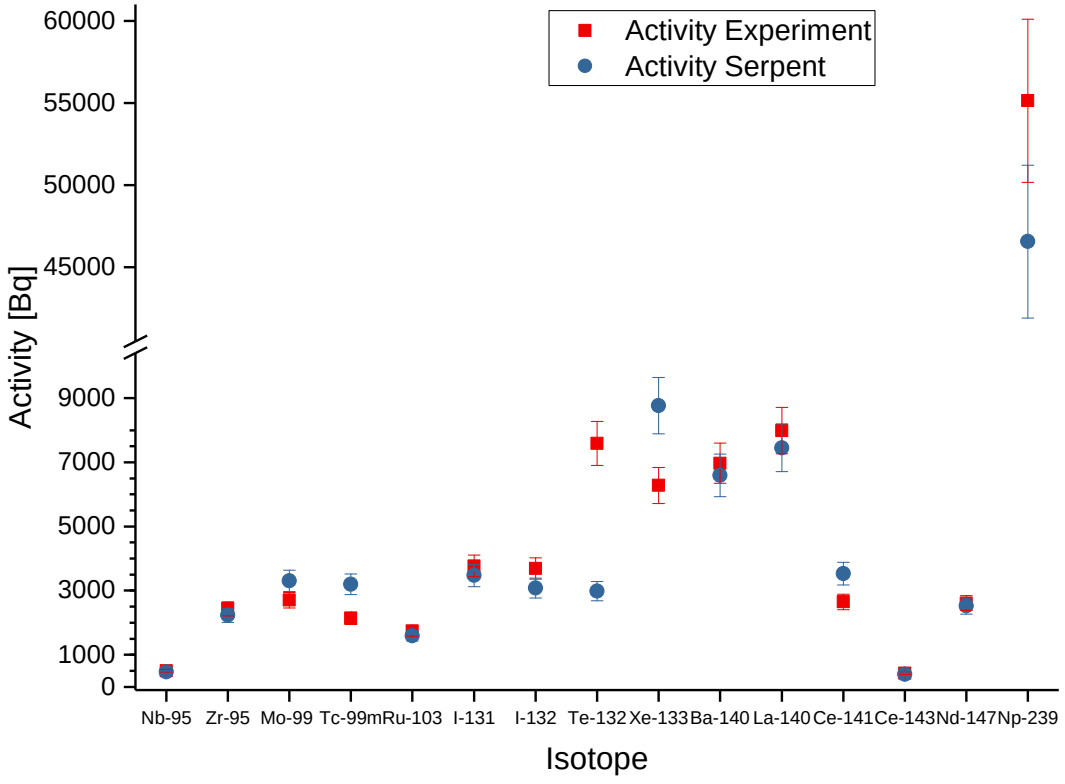

Figure 5.3.2: Activities of the Uranium-foil 11.13 days after the irradiation

By the Gamma Spectroscopy of the Thorium foil only four isotopes are found, three with low activities under 500 Bq; comparison of Serpent and experimental values are shown in figure 5.3.3.

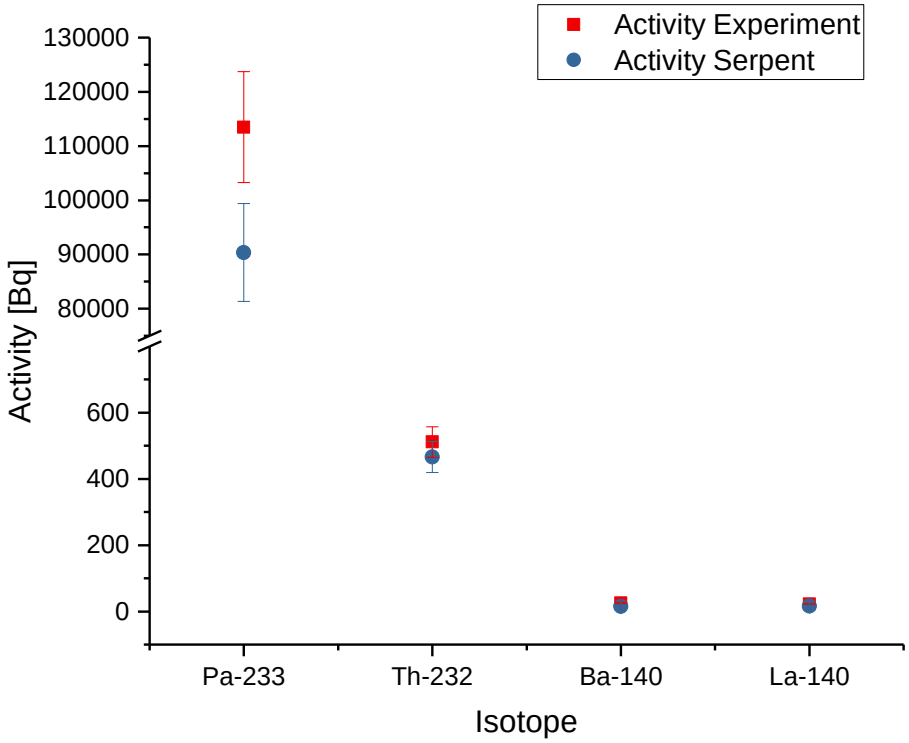

Figure 5.3.3: Activities of the Thorium-foil 7.73 days after the irradiation

5.4 Discussion of the Results

For the Uranium foil most determined activities are in a good agreement (below 10 %) between Serpent and the Experiment. But few isotopes have a big discrepant between the data obtained from the simulation and the experiment. This can be explained for the isotopes Tc-99m, Ce-141, Te-132 and Xe-133 with their γ-peak in low energy areas, between 0 and 230 keV. In this range, the efficiency calibration curve of the detector presents the bigger uncertainty. This can explain the large discrepancies of these isotopes. However, most isotopes are comparable, since they are in the range of uncertainties.

Comparing the data of the Thorium foil from the Serpent simulation with the data from the

experiment, the matching varies in a range of 8-40 %. This is not as good as the results with the Uranium foil. With Serpent the uncertainty in these low activity areas is higher than when considering higher activities. In the experiment, low activity also has higher uncertainty.

When comparing the results of the simulation with experimental data, one must be aware that the simulation has large inaccuracies. First it was demonstrated (see figure 4.3.7, that Serpent flux becomes less accurate moving to the outer core regions. The experimental position LS 1, is located out of the core in the graphite reflector. Second Serpent calculation in thin and small volumes is not accurate as in larger volumes. The foils are relatively thin so the calculation is not very precise [23]. The third inaccuracy is that the experimental set up was modelled with some geometrical approximations. There is no plastic cover over the foil, which is normally needed to inject the samples in the irradiation tube. The irradiation tube is as well just modelled with air, when in reality there is an aluminium tube.

Chapter 6

Nuclide Determination of irradiated TRIGA Fuel Elements

This chapter describes burn up simulation of the TRIGA Mark II fuel elements in Vienna. The determined data about the nuclide determination of these fuel elements were compared with data from gamma-spectroscopy measurements of several selected fuel elements in the year 2015. For this purpose, the activities of some fission products were compared. The fuel elements were inside the reactor core from the end of the year 2012 till April 2015. The measurements of the gamma spectroscopy of the fuel elements was preformed in December 2015.

6.1 Description of the Experiments

To obtain the activity of the fuel element of the TRIGA research reactor in Vienna, some irradiated fuel elements were measured using gamma spectroscopy in December 2015.
The investigated fuel elements were scanned along their vertical axis. For a safe measurement procedure the fuel elements were transferred inside the reactor tank into a special cask made of lead. It was then lifted from the reactor tank into the fuel scanning machine (FSM). The FSM was developed at the Atominstitut of the Technical University Vienna and it allows the optical and spectrometry inspection of TRIGA Mark II fuel elements. The γ-rays from the fuel element are bundled by a collimator to a gamma detector. The FSM can control the position of the fuel element with tine regulation (1 mm). The fuel element was lifted up to a level of 580 mm, this marks the bottom of the fuel element. It was then moved downwards and a gamma spectra measured every 10 mm. This gives a set of data along the vertical axis of the fuel element.

The used detector was a high purity germanium detector (HPGe detector). A schematic view of the experiment set up and the used distances can be found in the figures 6.1.1 and 6.1.2 [4].

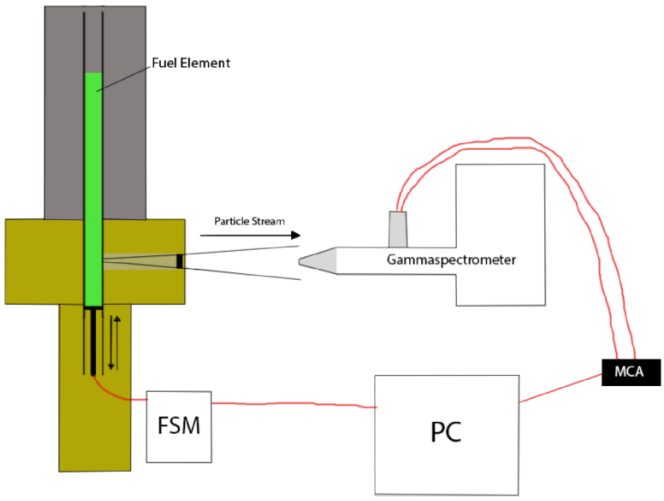

Figure 6.1.1: Schematic set up of the experiment [4]

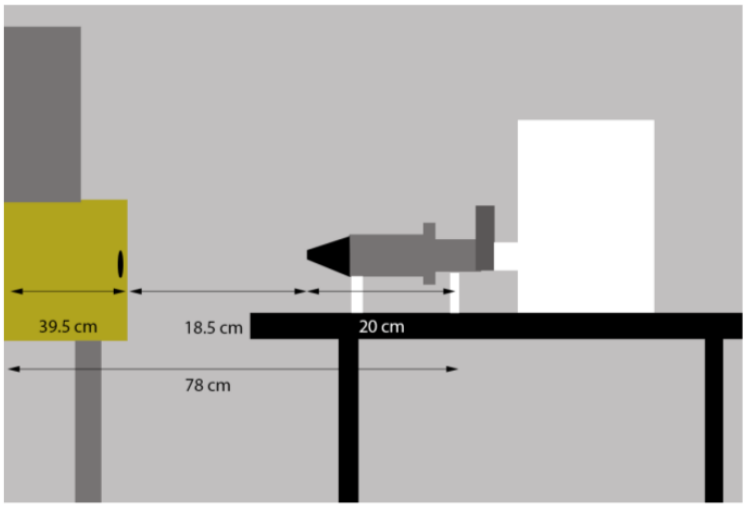

Figure 6.1.2: Schematic overview of the experiment and the used distances [4]

Because of the hight count rates, the Multi Channel Analyzer (MCA) was used. The MCA rejects electronic noise and background radiation and converts the analog signal into a digital one. Signals with similar energy are separated into groups, these groups are separated in

channels. For detailed results 8192 channels were used [26]. Six fuel elements from the current reactor core were measured. The last day of operation of the TRIGA research reactor was the 25. March 2015. The measurement takes place in December 2015, after aproper cooling period. The most active isotopes found were Cs-137, Co-60, Zr-95 and Ce-144. The results of the Zr-95 isotopes were in a way corrected, that the activities are only from the fission products. The following table list the investigated fuel elements from the core [4].

FE No	**Date of last Irradiation**	**Date of Measurement**	**Position in the Core**
9213	25. 03. 2015	01. 12. 2015	B2
9214	25. 03. 2015	02. 12. 2015	B4
9200	25. 03. 2015	02. 12. 2015	B1
9905	25. 03. 2015	03. 12. 2015	C1
9915	25. 03. 2015	03. 12. 2015	D1
9932	25. 03. 2015	03. 12. 2015	E1

Table 6.1.1: Measured Fuel Elements [26]

6.2 Serpent Simulation

To obtain the data from the Serpent Simulation burn up calculation were carried out.

6.2.1 Simulation 1: Burn up in 91 Days

To get a first estimation a simulation was carried out to simulated the burn up, between the fuel element change in the end of 2012 and the shut down of the reactor for a new instrumentation set up in April 2015. The start of the normal operation of the reactor was the 21. January 2013, between this date and the 1. April 2015 the cumulative work of the reactor in this time interval was:

$$W_{21.01.13-01.04.25} = 547.841 \ \ MWh$$

This value was estimated from the logbooks of the reactor operation.
As a simplification it was assumed that the reactor operated with a full power of 250 kW continuously. This would correspond to a period of 91.31 days of operation till the cumulative work of the reactor is reached.
The option of this calculation are presented in table 6.2.1.

Source neutron per cycle	1 000 000
Number of cycles	1500
Power	250000 W
Burn up time	91.307 days
Method for depletion calculation	Transmutation Trajectory Analysis (TTA)
Optimization	maximal performance
Unresolved resonance probability tables	in use
Position of burned fuel elements	B2, B4 C1, D1 and E1

Table 6.2.2: Burn up Option

6.2.2 Results from the Nuclide Determination of the Fuel Elements and the Serpent Simulation 1

The most likely fission products were calculated with Serpent and their activities are shown in table 6.2.3. Also the total Activity of every selected fuel element is shown in this table.

	B2-9213	**B4-9214**	**C1-9905**	**D1-9915**	**E1-9932**
Isotope	**Activity** [Bq]	**Activity** [Bq]	**Activity** [Bq]	**Activity** [Bq]	**Activity** [Bq]
Cs-137	$5.80 \cdot 10^{10}$	$5.49 \cdot 10^{10}$	$4.66 \cdot 10^{10}$	$3.96 \cdot 10^{10}$	$3.12 \cdot 10^{10}$
Ce-144	$1.79 \cdot 10^{12}$	$1.69 \cdot 10^{12}$	$1.43 \cdot 10^{12}$	$1.22 \cdot 10^{12}$	$9.61 \cdot 10^{11}$
Zr-95	$6.65 \cdot 10^{12}$	$6.30 \cdot 10^{12}$	$5.34 \cdot 10^{12}$	$4.55 \cdot 10^{12}$	$3.58 \cdot 10^{12}$
Sr-90	$5.65 \cdot 10^{10}$	$5.35 \cdot 10^{10}$	$4.54 \cdot 10^{10}$	$3.86 \cdot 10^{10}$	$3.04 \cdot 10^{10}$
Nb-95	$3.99 \cdot 10^{12}$	$3.78 \cdot 10^{12}$	$3.21 \cdot 10^{12}$	$2.73 \cdot 10^{12}$	$2.15 \cdot 10^{12}$
Mo-99	$9.90 \cdot 10^{12}$	$9.38 \cdot 10^{12}$	$7.96 \cdot 10^{12}$	$6.78 \cdot 10^{12}$	$5.34 \cdot 10^{12}$
Tc-99	$7.79 \cdot 10^{6}$	$7.37 \cdot 10^{6}$	$6.25 \cdot 10^{6}$	$5.32 \cdot 10^{6}$	$4.19 \cdot 10^{6}$
Ru-103	$3.97 \cdot 10^{12}$	$3.76 \cdot 10^{12}$	$3.19 \cdot 10^{12}$	$2.72 \cdot 10^{12}$	$2.14 \cdot 10^{12}$
Te-132	$6.98 \cdot 10^{12}$	$6.61 \cdot 10^{12}$	$5.61 \cdot 10^{12}$	$4.78 \cdot 10^{12}$	$3.76 \cdot 10^{12}$
I-131	$4.69 \cdot 10^{12}$	$4.44 \cdot 10^{12}$	$3.77 \cdot 10^{12}$	$3.21 \cdot 10^{12}$	$2.53 \cdot 10^{12}$
I-133	$1.09 \cdot 10^{13}$	$1.03 \cdot 10^{13}$	$8.73 \cdot 10^{12}$	$7.44 \cdot 10^{12}$	$5.86 \cdot 10^{12}$
I-135	$1.02 \cdot 10^{13}$	$9.65 \cdot 10^{12}$	$8.19 \cdot 10^{12}$	$6.98 \cdot 10^{12}$	$5.50 \cdot 10^{12}$
Xe-133	$1.09 \cdot 10^{13}$	$1.03 \cdot 10^{13}$	$8.74 \cdot 10^{12}$	$7.45 \cdot 10^{12}$	$5.86 \cdot 10^{12}$
Ba-140	$1.00 \cdot 10^{13}$	$9.49 \cdot 10^{12}$	$8.05 \cdot 10^{12}$	$6.86 \cdot 10^{12}$	$5.40 \cdot 10^{12}$
La-140	$1.00 \cdot 10^{13}$	$9.50 \cdot 10^{12}$	$8.05 \cdot 10^{12}$	$6.86 \cdot 10^{12}$	$5.40 \cdot 10^{12}$
Pr-144	$1.79 \cdot 10^{12}$	$1.69 \cdot 10^{12}$	$1.44 \cdot 10^{12}$	$1.22 \cdot 10^{12}$	$9.62 \cdot 10^{11}$
Nd-147	$3.63 \cdot 10^{12}$	$3.44 \cdot 10^{12}$	$2.92 \cdot 10^{12}$	$2.49 \cdot 10^{12}$	$1.96 \cdot 10^{12}$
Pm-147	$1.94 \cdot 10^{11}$	$1.84 \cdot 10^{11}$	$1.56 \cdot 10^{11}$	$1.33 \cdot 10^{11}$	$1.04 \cdot 10^{11}$
total Activity	$9.18 \cdot 10^{14}$	$8.73 \cdot 10^{14}$	$7.43 \cdot 10^{14}$	$6.33 \cdot 10^{14}$	$4.98 \cdot 10^{14}$

Table 6.2.3: Isotope Activity of the burned fuel elements calculated with Serpent

This is the total fuel element activity. Each investigated fuel element was divided in 38 parts along the z-axis to get the vertical distribution of the activity. Serpent gave a material output after each burn up step for all burned materials in 38 parts. These files consist of the material composition of all isotopes in atomic density (unit $10^{24}/cm^3$). Multiplied by the volume of this part of the fuel element, it surrendered the total number of nuclides in this part, with equation 1.17 the activity of the parts of the fuel element can be calculated. In the following figure 6.2.3 the Cs-137 activity distribution for the five fuel elements along the z-axis are shown.

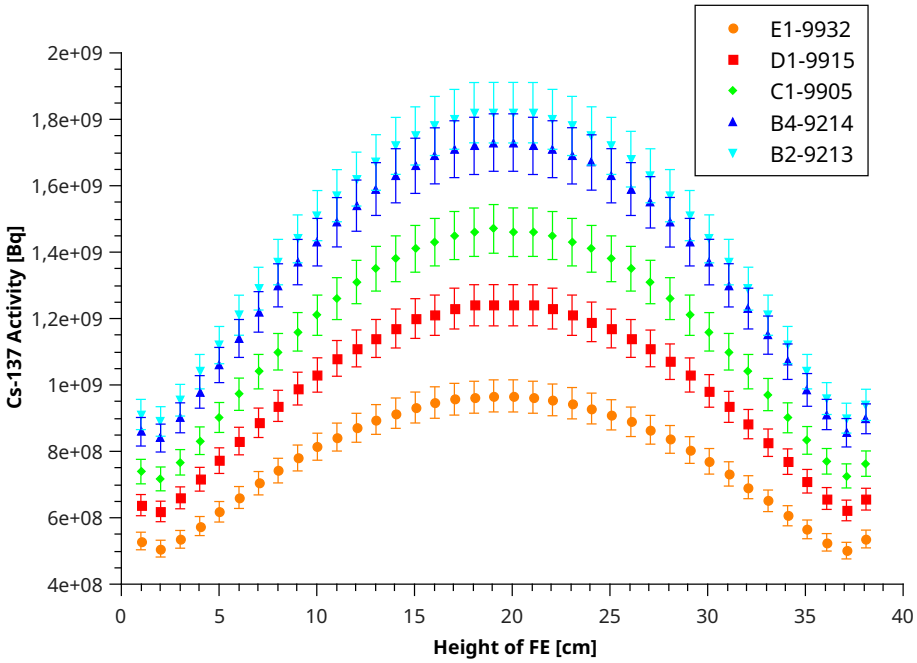

Figure 6.2.3: Cs-137 Activity along the z-axis in the different FE obtained with Serpent

The results of the simulations were compared with the data from the gamma spectroscopy of the fuel elements. The activities of isotopes Cs-137, Ce-144 and Zr-95 were compared with each other. The data from the measurements was first compared with the results from simulation 1. This comparison is shown in the following figures 6.2.4. The data from the fuel element B1 are not in the comparison, because this element was part of the reactor before the new core was loaded in the year 2012. The core configuration was very different at that time, i.e. it is not possible to evaluate its inventory with the current core calculation. The total activities of all fuel elements from the measurements and from the simulation can be found in the table 6.2.4. The uncertainties are approximately 5 % for the Cs-137 isotope and 10 % for Ce-144.

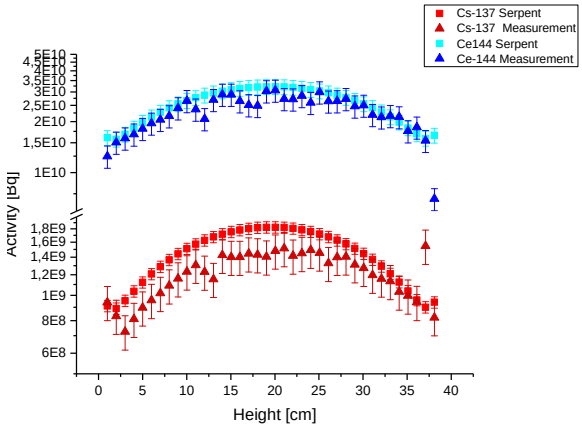

(a) Fuel Element B2-9213

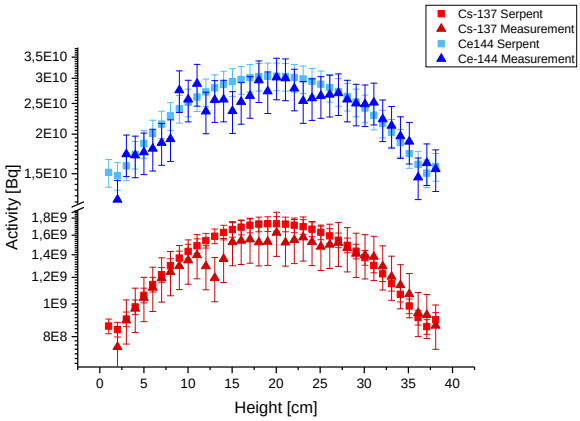

(b) Fuel Element B4-9214

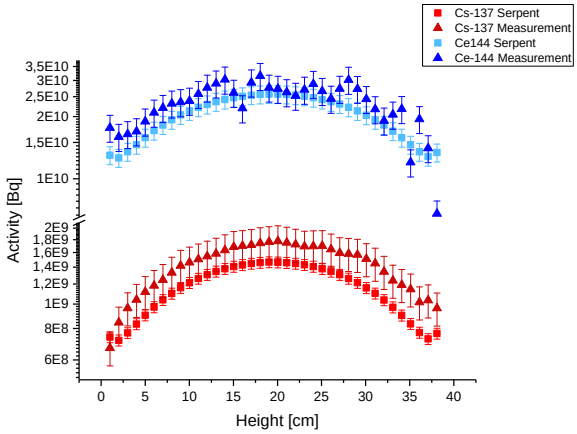

(c) Fuel Element C1-9905

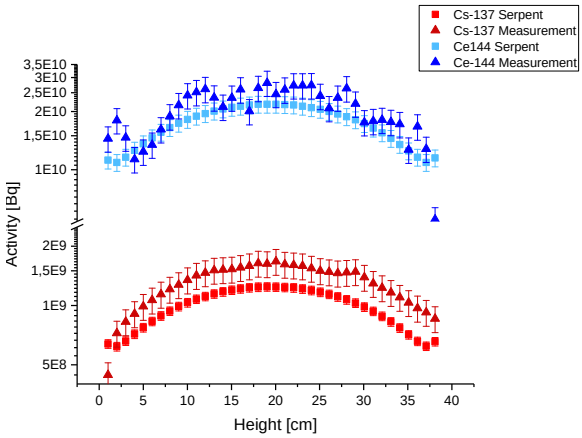

(d) Fuel Element D1-9915

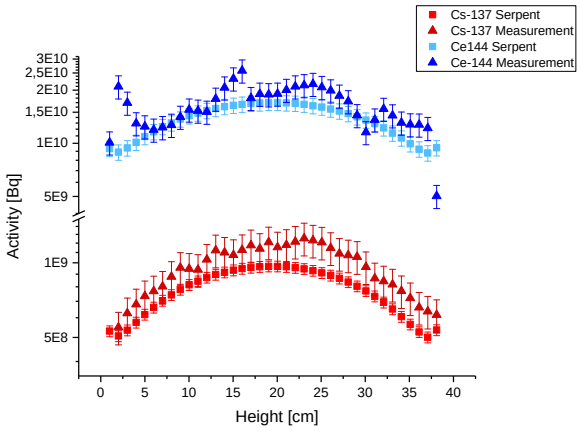

(e) Fuel Element E1-9932

Figure 6.2.4: Compared Activities of the isotopes Cs-137 and Ce-144 from the measurements (triangle) and the Serpent Simulation 1 (squares)

	Cs-137 Activity [Bq]		**Ce-144 Activity [Bq]**		**Zr-95 Activity [Bq]**	
	Measurement	Serpent	Measurement	Serpent	Measurement	Serpent
B2-9213	$4.62 \cdot 10^{10}$	$5.47 \cdot 10^{10}$	$8.71 \cdot 10^{11}$	$9.64 \cdot 10^{11}$	$1.27 \cdot 10^{11}$	$4.37 \cdot 10^{11}$
B4-9214	$4.88 \cdot 10^{10}$	$5.19 \cdot 10^{10}$	$8.67 \cdot 10^{11}$	$9.13 \cdot 10^{11}$	$1.18 \cdot 10^{11}$	$4.10 \cdot 10^{11}$
C1-9905	$5.38 \cdot 10^{10}$	$4.39 \cdot 10^{10}$	$8.79 \cdot 10^{11}$	$7.71 \cdot 10^{11}$	$9.35 \cdot 10^{10}$	$3.44 \cdot 10^{11}$
D1-9915	$4.92 \cdot 10^{10}$	$3.74 \cdot 10^{10}$	$7.71 \cdot 10^{11}$	$6.57 \cdot 10^{11}$	$8.66 \cdot 10^{10}$	$2.93 \cdot 10^{11}$
E1-9932	$3.56 \cdot 10^{10}$	$2.94 \cdot 10^{10}$	$6.18 \cdot 10^{11}$	$5.17 \cdot 10^{11}$	$6.24 \cdot 10^{10}$	$2.30 \cdot 10^{11}$

Table 6.2.4: Total Activities of the investigated Fuel Elements

In figure 6.2.2 it can be seen that the data from the simulation are comparable with the obtained data from the experiment for the isotopes Cs-137 and Ce-144. The isotope Zr-95 was also measured and compared to the data of the simulation, this can be seen in the following figure 6.2.5. The uncertainty for this isotope is 15 %. This figure represents the data of the fuel element B2-9213. The big discrepancy between the results of the simulation and the experiments are in the other fuel elements the same and, considering the Zr-95 half life ($T_{1/2}$=64 days), it was expected Serpent to overestimate the activity value.

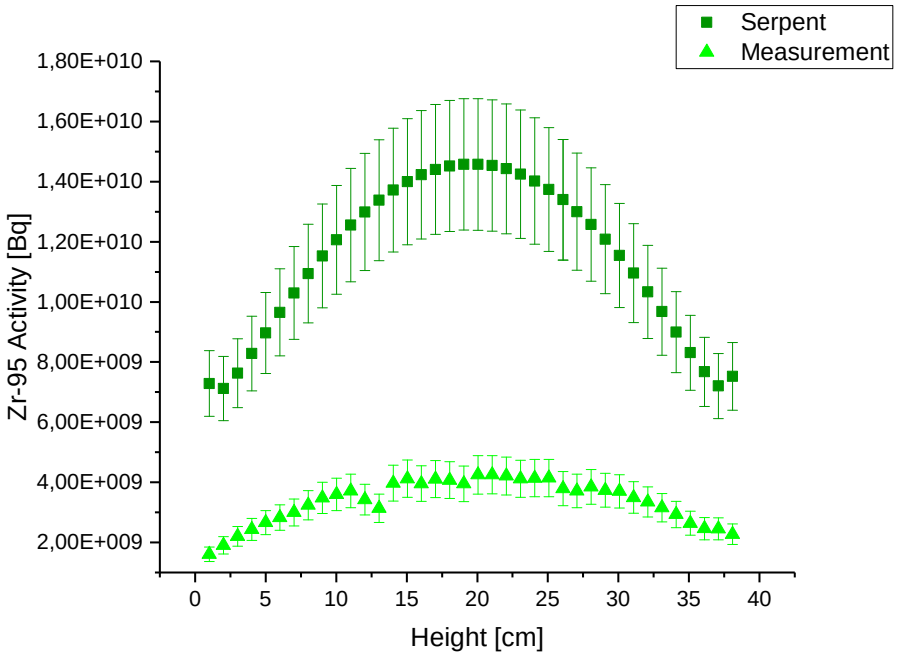

Figure 6.2.5: Zr-95 Activity in Fuel Element B2-9213 obtain by the measurements (light green triangle) and Serpent (dark green square)

6.2.3 Discussion of the Results from the Nuclide Determination of the Fuel Elements

6.2.3.1 Caesium Distribution in the Fuel Elements

For the fuel elements 9213 and 9214 at the Positions B2 and B4 the activity of Cs-137 is higher in the Serpent simulation. For the other three elements the measured activity is higher than the one from Serpent. The differences are about 20 %.
This can be explained by the fact that the history of the elements is different. The fuel elements 9213 and 9214 were fresh fuel elements set in the core during the core configuration in 2012. The fuel elements 9905, 9915 and 9932 are fuel elements which were used before in Japan till 1989. During the time in Japan Caesium 137 was produced and it is not totally decayed up to this date. This is the reason for the higher Cs-137 concentration in these fuel elements. In the simulation fresh elements were assumed, as no detailed burn up or inventory data were made available for these fuel elements. So the output is just the isotopes which were built up during the reactor run in Vienna.

6.2.3.2 Cerium Distribution in the Fuel Elements

The half-life of the Cerium isotope Ce-144 is 284.91 days [25]. The fuel elements from the Japanese reactor Musashi had last been used in Japan in 1989. Therefore all Ce-144 in the fuel elements from that time ad already decayed. The measured activity of Ce-144 comes only from the produced Ce-144 in the reactor in Vienna.
Comparing the activities from the measurements with those from the simulation, the discrepancies of the total activities for all fuel elements lie between 5-16 %. The worst match was the outermost fuel element E1-9932 with 16%, the best match was B4-9214 with 5 %. Also the individual data along the vertical direction are on average below 10% deviation. The Serpent simulation is thus a good tool to simulate the data for the Ce-144 activities in the fuel element.

6.2.3.3 Zirconium Distribution in the Fuel Elements

The values of the total activities of the Zr-95 isotope are 50% higher for all fuel elements in the Serpent simulation than the measured activities, see figure 6.2.4. The half-life of Zr-95 is 94.91 days. The half-life is so short that no isotopes from reactor operation in Japan are any more present in the fuel elements. Despite this half-life is nearly the same as the burn up time in Simulation 1, the real operation time was over three years, so the

produced Zr-95 decays during the operation time. This is not considered in the simulation 1 to ensure the activity is too high. The data from the Zr-95 activity of this Serpent simulation cannot provide a significant statement. For that the parameters of the simulation have to be changed.

6.3 Changing the Parameter of the Serpent Simulation

To simulate the short-life isotopes in an more accurate way the parameters of the simulation were changed. Using the example of the Zr-95 isotope, the results of the various simulations were compared. The first simulation described in the previous section 6.2.1 are also considered as Simulation 1. The compared time of the activity was 251 days (till December 2015) after the shut down of the reactor in April 2015. This time interval was chosen, to compare the results with experimental data, for which a cool down time of several months is needed.

6.3.1 Simulation 2 - average power

In this simulation the real time was assumed and the simulation was carried out for the time interval from 1. April 2014 till 1. April 2015. Twelve months divided in steps, each step with a burn up time of two months. The cumulative work for each two months period was taken again from the handbooks of the reactor operator. Then the average power was calculated. This means it was simulated that the reactor operates the total time by a low power. Just the last twelve months of operation were considered, because the Zr-95 amount from January 2013 till April 2014 is decayed, at the time of measurement in December 2015. The average power of the steps and the parameters of this burn up simulation can be found in the table 6.3.5 below.

Source neutron per cycle	1 000 000
Number of cycles	1500
Method for depletion calculation	Transmutation Trajectory Analysis (TTA)
Optimization	maximal performance
Unresolved resonance probability tables	in use
Position of burned fuel elements	B2, B4 C1, D1 and E1

Table 6.3.5: Burn up Parameters for the Simulation 2

Step	Days [d]	Power [kW]
1	62	35.39
2	60	33.04
3	61	22.25
4	61	25.90
5	63	16.23
6	58	29.76
7	251	0

Table 6.3.6: Irradiation History of Simulation 2

6.3.1.1 Results and Comparison of the Measurements with Simulation 2

In simulation 2 the real time was modelled, but an average power was used. The results compared with the experimental data are shown in figure 6.3.6. The total Zr-95 activities from the simulation and the measurements are listed in table 6.3.7.

	Zr-95 Activity [Bq]		
	Measurement	Serpent	Difference
B2-9213	$1.27{\cdot}10^{11} \pm 1.91{\cdot}10^{10}$	$6.95{\cdot}10^{10} \pm 1.04{\cdot}10^{10}$	45.46 %
B4-9214	$1.18{\cdot}10^{11} \pm 1.77{\cdot}10^{10}$	$6.59{\cdot}10^{10}$ $9.89{\cdot}10^{9}$	44.24 %
C1-9905	$9.35{\cdot}10^{10} \pm 1.40{\cdot}10^{10}$	$5.58{\cdot}10^{10}$ $8.37{\cdot}10^{9}$	40.34 %
D1-9915	$8.66{\cdot}10^{10} \pm 1.30{\cdot}10^{10}$	$4.74{\cdot}10^{10}$ $7.11{\cdot}10^{9}$	45.20 %
E1-9932	$6.24{\cdot}10^{10} \pm 9.36{\cdot}10^{9}$	$3.74{\cdot}10^{10}$ $5.61{\cdot}10^{9}$	40.12 %

Table 6.3.7: Total Activities of the investigated Fuel Elements of Simulation 2 compared to the Results of the Experiments

In this case the values of the Serpent simulation are lower than the measurements. The difference between them is 40-45 %. In the simulation the reactor power is lower than in real, because of this the production rate of fission products is lower. This is the reason for this big discrepancy. To avoid this, but nevertheless to choose the correct time another simulation was performed.

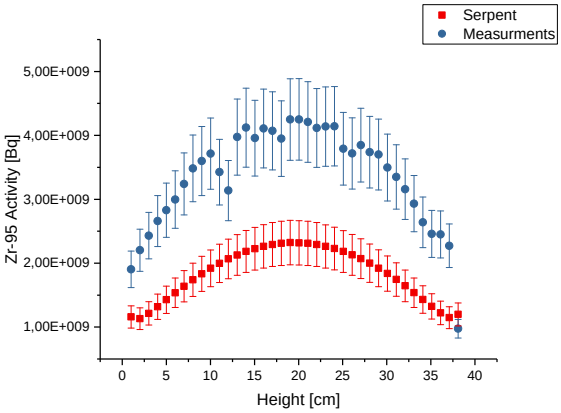

(a) Fuel Element B2-9213

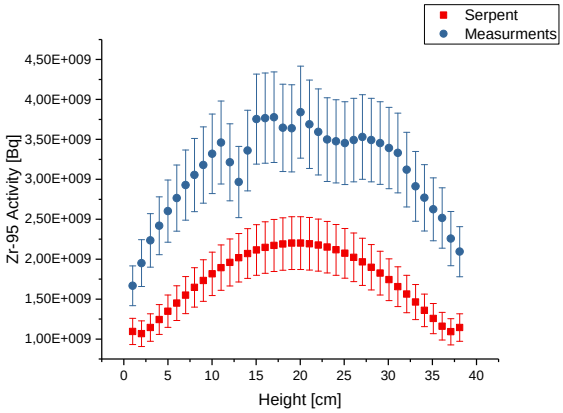

(b) Fuel Element B4-9214

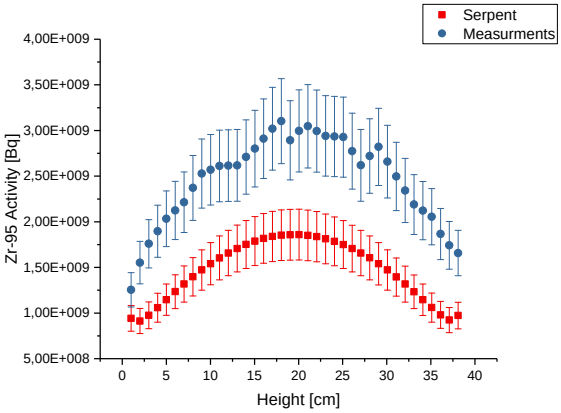

(c) Fuel Element C1-9905

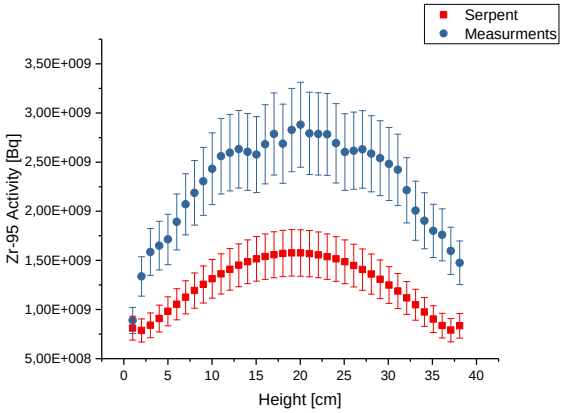

(d) Fuel Element D1-9915

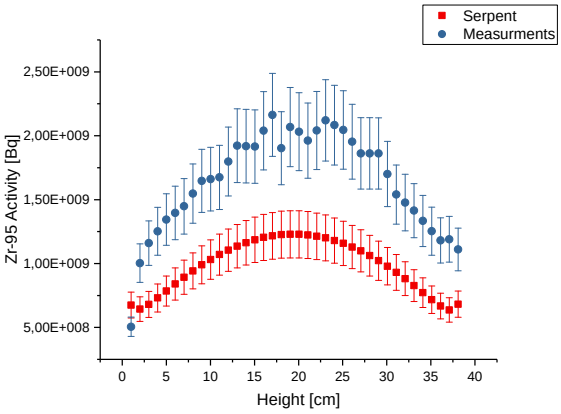

(e) Fuel Element E1-9932

Figure 6.3.6: Compared Activities of the isotope Zr-95 from the measurements (blue) and the Serpent Simulation 2 (red)

6.3.2 Simulation 3 - 12 month of operation in two month intervals

In this simulation the reactor operates with the normal power of 250 kW. To simulated the time in which the Zr-95 is decayed, the simulation is divided into several steps in which the reactor power is set at 0 kW. Again only the last twelve months of reactor operation were used due to the same reason mentioned above.
Two month of operation were set together in an interval. The days of irradiating were placed in the end of the two month period. These days corresponding to the calculated reactor work in the 2 month interval. For the remaining days the power of the reactor was set at 0 kW. So each interval has two burn up steps. With this method the real time was simulated and the real power.
To define the steps the cumulative work for two month were taken from the logbooks of the reactor operator. The corresponding time for the simulation was April 2014 till April 2015. The last step (251 days) was the time from April 2015 till December 2015 were the reactor was shut down. The time used for the intervals can be found in the table 6.3.8

Interval	**Dates**
1	01.04.2014 - 02.06.2014
2	03.06.2014 - 01.08.2014
3	02.08. 2014 - 01.10.2014
4	02.10.2014 - 01.12.2014
5	02.12.2014 - 02.02.2015
6	03.02.2015 - 01.04.2015

Table 6.3.8: Dates of the intervals

Each interval consist of two burn up steps, in the first step the work of the reactor is defined and the second steps is simulate the decay time. A summary of the parameters of this simulation can be found in the table below 6.3.9.

Source neutron per cycle	1 000 000
Number of cycles	1500
Method for depletion calculation	Transmutation Trajectory Analysis (TTA)
Optimization	maximal performance
Unresolved resonance probability tables	in use
Position of burned fuel elements	B2, B4 C1, D1 and E1

Table 6.3.9: Burn up Parameters for the Simulation 3

Step	Days [d]	Power [kW]
1	8.8	250
2	53.2	0
3	7.9	250
4	52.1	0
5	5.4	250
6	55.6	0
7	6.3	250
8	54.7	0
9	4.1	250
10	58.9	0
11	6.9	250
12	251	0

Table 6.3.10: Irradiation History of Simulation 3

6.3.2.1 Results and Comparison of the Measurements with Simulation 3

Zr-95 was produced during the time in which the power was set at 250 kW, followed by a time of decay. This up-and-down movement of the total Zr-95 activity during the simulation can be seen in the following figure 6.3.7.

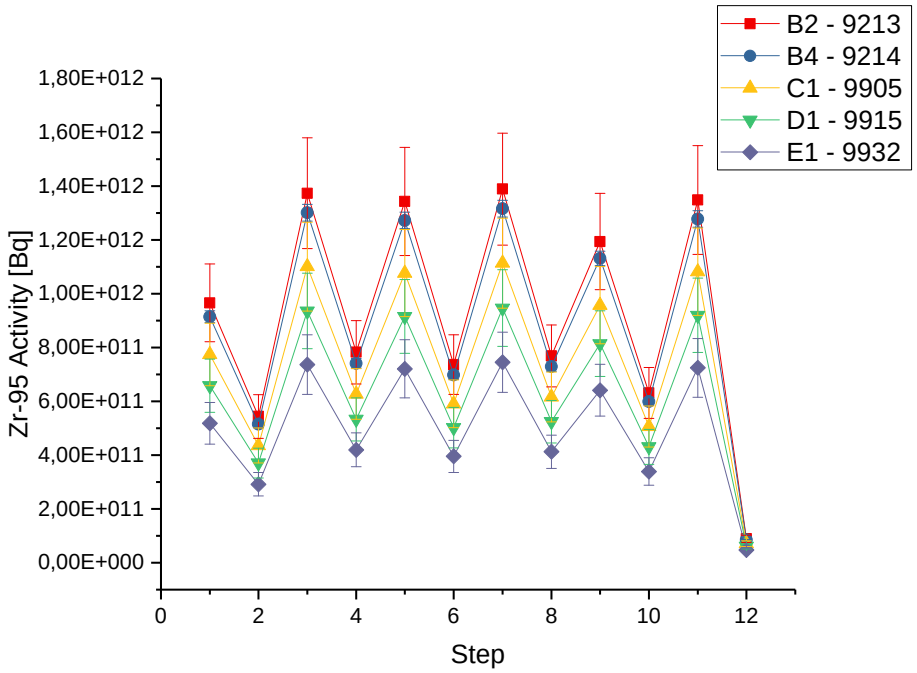

Figure 6.3.7: total Zr-95 Activity of the Fuel Elements after each burn up Step

The obtained Zr-95 activities are shown in figure 6.3.8 together with the obtained measurement results.

	Zr-95 Activity [Bq]		
	Measurement	Serpent	Difference
B2-9213	$1.27{\cdot}10^{11} \pm 1.91{\cdot}10^{10}$	$8.91{\cdot}10^{10} \pm 1.34{\cdot}10^{10}$	29.84 %
B4-9214	$1.18{\cdot}10^{11} \pm 1.77{\cdot}10^{10}$	$8.44{\cdot}10^{10} \pm 1.27{\cdot}10^{10}$	28.47 %
C1-9905	$9.35{\cdot}10^{10} \pm 1.40{\cdot}10^{10}$	$7.14{\cdot}10^{10} \pm 1.07{\cdot}10^{10}$	23.64 %
D1-9915	$8.66{\cdot}10^{10} \pm 1.30{\cdot}10^{10}$	$6.08{\cdot}10^{10} \pm 9.12{\cdot}10^{9}$	29.79 %
E1-9932	$6.24{\cdot}10^{10} \pm 9.36{\cdot}10^{9}$	$4.78{\cdot}10^{10} \pm 7.17{\cdot}10^{9}$	23.40 %

Table 6.3.11: Total Activities of the investigated Fuel Elements of Simulation 3 compared to the Results of the Experiments

The results from the Serpent simulation are again lower than the ones from the measurements. The discrepancies are around 30 % for the total activity in all fuel elements. This difference can be explained by the irradiation history of the simulation. In the simulation the entire power of two months was taken within a few days, the remaining time the reactor was turned off. However, this does not correspond to the reality in which the reactor is operating daily for several hours and is only switched off at night and on weekends. In reality,

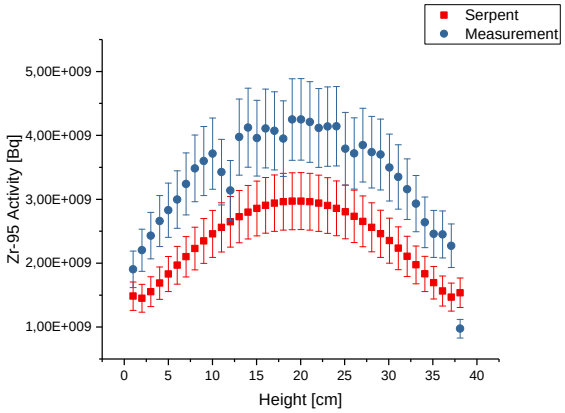

(a) Fuel Element B2-9213

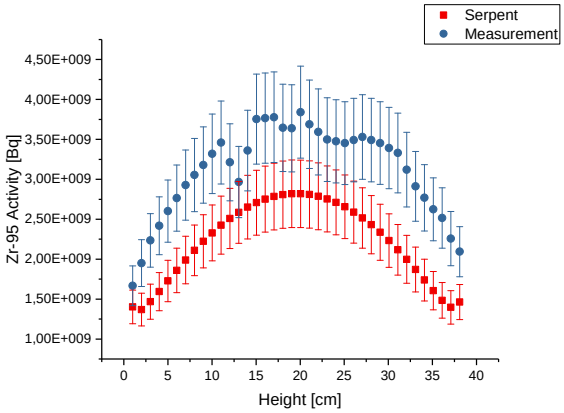

(b) Fuel Element B4-9214

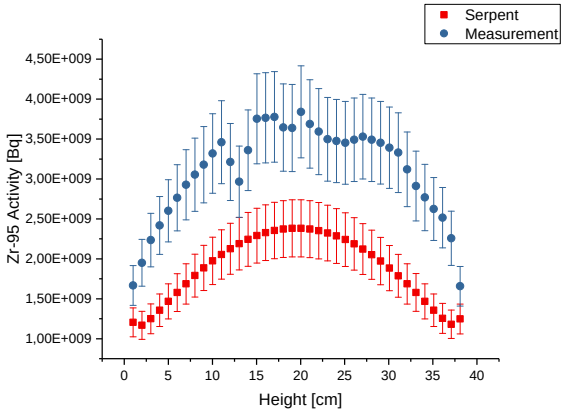

(c) Fuel Element C1-9905

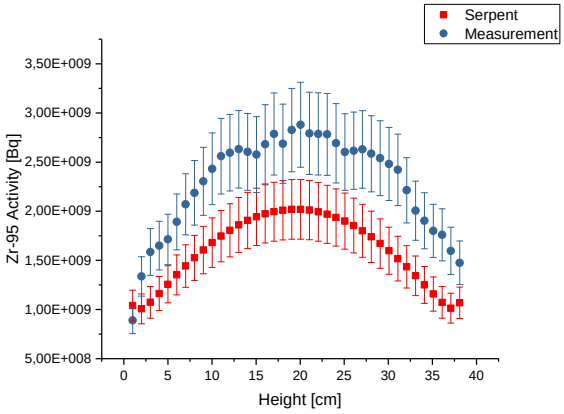

(d) Fuel Element D1-9915

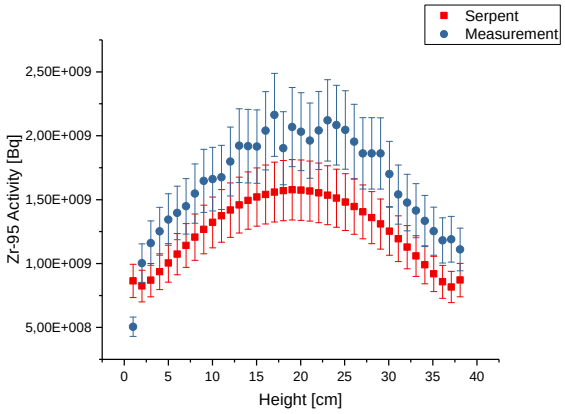

(e) Fuel Element E1-9932

Figure 6.3.8: Compared Activities of the isotope Zr-95 from the measurements (blue) and the Serpent Simulation 3 (red)

zirconium is produced daily, in simulation only during few days.

Simulation 3 is the best guess of these three different simulations. Nevertheless, even for this simulation many assumptions are made and it does not represent the real irradiation history. To get more accurate values for isotopes with half-lives like Zr-95 a more detailed irradiation history is needed. The problem with research reactors like the TRIGA Mark II in Vienna is, that they are shut down every evening so the history is changing daily and therefore a detailed simulation needs a lot of steps and with this a lot of calculation time.

Chapter 7

Burn up of the Fuel Elements

To investigate the burn up of the fuel elements during the reactor operation, the amount of uranium in the fuel elements before and after the simulation is compared. For this simulation the data from Simulation 1 is used, as the decay time is not important, because of the long half-life of uranium isotopes. The amount of uranium isotopes in mass fraction (unit $10^{24}/cm^3$) at the begin of the simulation (compared to the real date of January 2013) and the end of the simulation (April 2015) can be found in the table 7.0.1 the uncertainty of this results are about 10 %.

The Plutonium production always accurate as in this kind of reactors is small. It has to be considered that the starting values are not correct, the simulations were performed with fresh fuel elements. So the results are not the real total amounts of Uranium and Plutonium, but the relative change of these amounts is comparable to reality.

Serpent calculates the burn up of each fuel element, these values can be found in the list below. Also the element burn up in percent corresponding to the U-235 can be calculated, by comparing the U-235 amount before and after the burn up. Both values can be found in table 7.0.2.

	B2-9213		**B4-9214**		**C1-9905**		**D1-9915**		**E1-9932**	
	Mass Fraction		**Mass Fraction**		**Mass Fraction**		**Mass Fraction**		**Mass Fraction**	
Isotope	Before	After	Before	After	Before	After	Before	After	Before	After
U-235	$2.55{\cdot}10^{-4}$	$2.51{\cdot}10^{-4}$	$2.55{\cdot}10^{-4}$	$2.51{\cdot}10^{-4}$	$2.55{\cdot}10^{-4}$	$2.52{\cdot}10^{-4}$	$2.55{\cdot}10^{-4}$	$2.53{\cdot}10^{-4}$	$2.55{\cdot}10^{-4}$	$2.53{\cdot}10^{-4}$
U-236	0.00	$6.23{\cdot}10^{-7}$	0.00	$5.96{\cdot}10^{-7}$	0.00	$5.10{\cdot}10^{-7}$	0.00	$4.35{\cdot}10^{-7}$	0.00	$3.40{\cdot}10^{-7}$
U-238	$1.02{\cdot}10^{-3}$	$1.02{\cdot}10^{-3}$	$1.02{\cdot}10^{-3}$	$1.02{\cdot}10^{-3}$	$1.02{\cdot}10^{-3}$	$1.02{\cdot}10^{-3}$	$1.02{\cdot}10^{-3}$	$1.02{\cdot}10^{-3}$	$1.02{\cdot}10^{-3}$	$1.02{\cdot}10^{-3}$
Pu-239	0.00	$2.81{\cdot}10^{-7}$	0.00	$2.92{\cdot}10^{-7}$	0.00	$2.66{\cdot}10^{-7}$	0.00	$2.26{\cdot}10^{-7}$	0.00	$1.72{\cdot}10^{-7}$
Pu-240	0.00	$1.58{\cdot}10^{-9}$	0.00	$1.61{\cdot}10^{-9}$	0.00	$1.27{\cdot}10^{-9}$	0.00	$9.21{\cdot}10^{-10}$	0.00	$5.45{\cdot}10^{-10}$
Pu-241	0.00	$1.40{\cdot}10^{-11}$	0.00	$1.47{\cdot}10^{-11}$	0.00	$1.05{\cdot}10^{-11}$	0.00	$6.45{\cdot}10^{-12}$	0.00	$2.92{\cdot}10^{-12}$

Table 7.0.1: Amount of Uranium and Plutonium isotopes before and at the end of the simulation.

	Burn up [Mwd/kgU]	**Burn up** [% U-235]
B2-9213	2.539 ± 0.254	1.56 ± 0.16
B4-9214	2.403 ± 0.240	1.48 ± 0.15
C1-9905	2.035 ± 0.204	1.25 ± 0.13
D1-9915	1.731 ± 0.173	1.07 ± 0.11
E1-9932	1.361 ± 0.136	0.84 ± 0.08

Table 7.0.2: Burn up of the fuel elements

The results in table 7.0.2 only represent the relative change during the operation in Vienna, the simulations were performed with fresh fuel elements, but some of the fuel elements inside the core already had a previous burn up of around 1 %.

Chapter 8

Conclusion

In this thesis, the development and validation of the Serpent model for the TRIGA Mark II reactor of the Technical University Vienna was described.
The first part of this work describes the development of the reactor model by the Monte Carlo reactor physics code Serpent. The geometry, material card and other options selected are shown in detail in chapter 4.1.

The following chapters describe the validation of the Serpent model. This was done by comparison of the calculated neutron flux and energy spectrum values with data from previously performed Simulations by the reactor MCNP model. The neutron fluxes were compared in four position in the radial direction, eleven positions in the vertical direction and inside of one fuel element.
Comparing the calculated data from the two simulation (Serpent and MCNP) they had a very good agreement, with differences mostly below 10 %. In radial direction the best agreement was in the core centre. Further outwards the differences got greater but were still in a good agreement. Inside of the investigated fuel element the difference between the two models is insignificant. Due to the good agreement it was shown that the Serpent model is validated for further simulations.

After the successful validation, the Serpent model was used to simulate an irradiation experiment and compare results with available experimental data. In this experiment natural Uranium- and Thorium foils were irradiated in the reactor and afterwards the activities of the fission products were measured. These experimental data were compared with the inventory list of Serpent after the burn up calculation. Despite of some isotopes, the compared activities were in good agreement (around 10 % discrepancies). This comparison also validated the Serpent burn up calculation.

The next experiment which was compared was the nuclide determination of irradiated fuel elements of the TRIGA Mark II reactor in Vienna. This was done for five fuel elements in different rings. The irradiation history was simulated and the activities of some fission products after the burn up calculation were compared with the experimental data. The compared isotopes have different half-lives and due to this fact the agreement between the simulation and the experiment were diverse. The discrepancies at the comparison at the isotopes Cs-137 were 20 % and for Ce-144 it was 5-16 %. For the isotope Zr-95 the discrepancies were quite hight: to obtain better results for this isotopes further burn up calculation with a finest burn up history were carried out. This led to a difference between simulation and experiment of 30 %.
To obtain really good results, also for short half-life isotopes (such as 20-60 days half-life), the irradiation history should be set to more detail. The TRIGA Mark II reactor in Vienna is a research reactor, operating just a few hours per day, and shut down during night and during the weekend. This leads to the fact that the steps for a very precise simulation have to be set very small. Weekly, or even better, daily steps would yield comparable results. Unfortunately this will increase the simulation time and is beyond the scope of this work.

The last part of the work was the burn up evaluation of the fuel element during the operation time in Vienna. As a result the burn up was between 0.8-1.6 % for the fuel elements. As expected the fuel element in the inner rings had a larger burn up then the one at the outer rings. The calculated burn up just represented the burn up due to the operation in Vienna reactor. In same cases the total burn up of the elements is higher, because they were loaded in the core not fresh, but underwent irradiation about 20 years before in another reactor. This fact affects calculation results for those fuel elements, in particular for the evaluation of long half-live fission products, such as Cs-137.

In Conclusion, comparing the results from the different Serpent simulations with experimental data and from simulation programs results it was demonstrated, that the Serpent reactor model is an useful tool for activity. Nuclides determination as well as burn up of individual fuel elements or of the total core.

Bibliography

[1] R. Khan. *Neutronics Analysis of the TRIGA Mark II Reactor Core and its Experimental Facilities*. PhD thesis, Vienna Unicersity of Technology, 2010.

[2] J. Leppänen. Introduction in SERPENT. `http://montecarlo.vtt.fi/index.htm`. last Accessed: 11. 10. 2016.

[3] S. Dal Cin. *Determination of changes in the composition of natural Uranium and Thorium samples by irradiation at the TRIGA Mark II research Reactor at the Atominstitut-Vienna*. Bachelorthesis, Technische Universität WIen - Atominsitut, 2015.

[4] D. Eichleitner. *Nuclide Determination of TRIGA Fuel Elements by Gamma Spectriscopy*. Bachelorthesis, Technische Universität Wien, 2015.

[5] K. Bethge, G. Walter, and B. Wiedemann. *Kernphysik- Eine Einführung*. Springer, Berlin, Heidelberg, 3. edition, 2008.

[6] M. Villa. Reaktorphysik-Vorlesungsskriptum. Technische Universität Wien, 2008.

[7] R. Nave. Fission and fusion can yield energy. `http://hyperphysics.phy-astr.gsu.edu/hbase/NucEne/nucbin.html`. last Accessed: 02. 12. 2016.

[8] T. Mayer-Kuckuk. *Kernphysik- Eine Einführung*. B.G. Teubner, Stuttgart, Leipzig, Wiesbaden, 7. edition, 2002.

[9] B. Povh, K. Rith, C. Scholz, and F. Zetsche. *Teilchen und Kerne- Eine Einführung in die physikalischen Konzepte*. Springer, Berlin, Heidelberg, New York, 6.auflage edition, 2004.

[10] C. Chieh. Fission Yield U-235. `https://sciborg.uwaterloo.ca/~cchieh/cact/nuctek/fissionyield.html`. last Accessed: 09. 12. 2016.

[11] M.B. Chadwick, M. Herman, P. Obložinský, et al. ENDF/B-VII.1 Nuclear Data for Science and Technology: Cross Sections, Covariances, Fission Product Yields and Decay Data. *Nuclear Data Sheets*, 112(12):2887 – 2996, 2011. Special Issue on ENDF/B-VII.1 Library.

[12] J. Leppänen. *Development of a New Monte Carlo Reactor Physics Code*. PhD thesis, Helsinki University of Technology, 2007.

[13] H. Böck, M. Villa, and R. Bergmann. Five Decades of TRIGA Reactor. In *NENE 25th International Confernce Nuclear Energy for New Europe*, 2016.

[14] M. Villa H. Böck, J. Razvi. History, Development and Future of TRIGA Research Reactors. Technical report, International Atomic Energy Agency, 2015.

[15] Nuclear Installation Safety Division of the IAEA. TRIGA Reactor Characteristics. https://ansn.iaea.org/Common/documents/Training/TRIGA%20Reactors%20%28Safety%20and%20Technology%29/chapter1/characteristics11.htm, April 2005. last Accessed: 10. 10. 2016.

[16] H. Böck and M. Villa. Praktische Übungen am Reaktor, Oktober 2005.

[17] Technische Universität Wien Atominsitut. Technische Daten des Reaktors. http://ati.tuwien.ac.at/reaktor/technische_daten/. last Accessed: 28. 10. 2016.

[18] M. Villa. Statusbericht TRIGA Reaktor Wien, 2013.

[19] M.Villa, R. Bergmann, A. Musilek, J. H. Sterba, and H. Böck amd C. Messick. The Core Conversion of the TRIGA Reactor Vienna. In *22nd International Conference Nuclear Energy for New Europe*, 2013.

[20] The TRIGA Mark-II Reaktor of the Atominstitut, Vienna, Austria. Vienna University of Technology.

[21] Querschnitt des TRIGA Mark-II Reaktors. http://ati.tuwien.ac.at/reaktor/querschnitt/. last Accessed: 10. 10. 2016.

[22] J. Leppänen. Development of SERPENT. http://montecarlo.vtt.fi/development.htm. last Accessed: 11. 10. 2016.

[23] J. Leppänen. Serpent - a Continuous-energy Monte Carlo Reactor Physics Burnup Calculation Code User's Manual, March 2007.

[24] M. Cagnazzo, T. Stummer, M. Villa, and H. Böck. Validation of the MCNP6 Model at the Atominstitut TRIGA Reactor. In *Research Reactor Fuel Management Conference (RRFM)*, 2015.

[25] Nudat 2.6. `http://www.nndc.bnl.gov/nudat2/`. last Accessed: 21. 01. 2017.

[26] D. Eichleitner, M. Cagnazzo, M. Villa, and H. Böck. Nuclide Determination of TRIGA Fuel Elements by Gamma Spectroscopy. In *Research Reactor Fuel Management Conference (RRFM)*, 2016.